MODELING AND CONTROL OF CONSTRAINED FLEXIBLE JOINT PARALLEL MANIPULATORS

A THESIS SUBMITTED TO
THE GRADUATE SCHOOL OF NATURAL AND APPLIED SCIENCES
OF
MIDDLE EAST TECHNICAL UNIVERSITY

BY

OSMAN CAN OĞAN

IN PARTIAL FULLFILMENT OF THE REQUIREMENTS
FOR
THE DEGREE OF MASTER OF SCIENCE
IN
MECHANICAL ENGINEERING

FEBRUARY 2010

Approval of the thesis:

MODELING AND CONTROL OF CONSTRAINED FLEXIBLE JOINT PARALLEL MANIPULATORS

submitted by **OSMAN CAN OĞAN** in partial fulfillment of the requirements for the degree of **Master of Science in Mechanical Engineering Department, Middle East Technical University** by,

Prof. Dr. Canan ÖZGEN
Dean, Graduate School of **Natural and Applied Sciences** _____

Prof. Dr. Süha ORAL
Head of Department, **Mechanical Engineering** _____

Prof. Dr. Kemal İder
Supervisor, **Mechanical Engineering Dept., METU** _____

Examining Committee Members

Prof. Dr. Kemal Özgören _____
Mechanical Engineering Dept., METU

Prof. Dr. Kemal İder _____
Mechanical Engineering Dept., METU

Prof. Dr. Reşit Soylu _____
Mechanical Engineering Dept., METU

Asst. Prof. Dr. Yiğit Yazıcıoğlu _____
Mechanical Engineering Dept., METU

Dr. Sinan Kılıçaslan _____
Mechanical Engineering Dept., Gazi University

Date: 1 February 2010

I hereby declare that all information in this document has been obtained and presented in accordance with academic rules and ethical conduct. I also declare that, as required by these rules and conduct, I have fully cited and referenced all material and results that are not original to this work.

Name, Last name : Osman Can Oğan

Signature :

ABSTRACT

MODELING AND CONTROL OF CONSTRAINED FLEXIBLE JOINT PARALLEL MANIPULATORS

OĞAN, Osman Can
M.S., Department of Mechanical Engineering
Supervisor: Prof. Dr. Kemal İder
February 2010, 81 pages

The purpose of the thesis is to achieve a hybrid force and motion control method of parallel manipulators working in a constrained environment, in the presence of joint flexibility that occurs at the actuated joints.

A flexible joint is modeled and the equations of motion of the parallel manipulator are derived by using the Lagrange formulation. The structural damping of the active joints, viscous friction at the passive joints and the rotor damping are also considered in the model. It is shown that in a flexible joint manipulator, the acceleration level inverse dynamic equations are singular because the control torques do not have instantaneous effect on the manipulator end-effector contact forces and accelerations due to the flexibility. Implicit numerical integration methods are utilized for solving the singular equations.

As a case study, a two legged constrained planar parallel manipulator with three degrees of freedom is simulated to illustrate the performance of the method.

Keywords: Parallel manipulator, flexible joint, inverse dynamics control

ÖZ

ESNEK EKLEMLİ KISITLANMIŞ PARALEL MANİPÜLATÖRLERİN MODELLEMESİ VE KONTROLÜ

OĞAN, Osman Can
Yüksek Lisans, Makine Mühendisliği Bölümü
Tez Yöneticisi: Prof. Dr. Kemal İder
Şubat 2010, 81 sayfa

Bu tezin amacı, eklem esnekliği göz önüne alınmış ve kısıtlı ortamlarda çalışan paralel manipülatörler için kuvvet ve hareket kontrolü sağlayacak bir kontrol metodu geliştirmektir.

Esnek bir eklem modellenmiş ve Lagrange formülasyonu kullanılarak paralel manipülatörün hareket denklemleri çıkarılmıştır. Aktif eklemlerdeki yapısal sönüm, pasif eklemlerdeki viskoz sürtünme ve eyletici rotorunun sönümü de dikkate alınmıştır. Bir esnek eklemli manipülatörde, kontrol torklarının esneklikten dolayı manipülatör ucundaki temas kuvvetleri ve ivmelere ani etki yapamadığı için, ivme seviyesindeki dinamik denklemlerin tekil olduğu gösterilmiştir. Tekil denklemlerin çözümü için kapalı nümerik integral metodoları kullanılmıştır.

Metodun performansını göstermek için, örnek olarak iki bacaklı, üç serbestlik dereceli, kısıtlanmış ve esnek eklemli düzelmsel bir paralel manipülatör ele alınmıştır.

Anahtar Kelimeler: Paralel manipülatörler, esnek eklem, ters dinamik kontrol.

ACKNOWLEDGMENTS

I wish to express my deepest appreciation to my supervisor Prof. Dr. Kemal İder for his supervision, advice, criticism, encouragements and insight throughout the thesis.

I would like to thank to my family for their love and support.

TABLE OF CONTENTS

LIST OF TABLES

TABLE OF FIGURES

CHAPTER 1

INTRODUCTION

1.1 Literature Survey

Parallel manipulators offer a closed-loop structure which yields some advantages in comparison to serial manipulators such as ability to carry heavier loads with greater accuracy and rigidity. The most common areas of application for parallel mechanisms are where high-load capability and high-motion accuracy are needed such as earthquake simulators and flight simulators. Moreover, planar parallel mechanisms are commonly used in micro-motion manipulators. Due to these advantages, parallel manipulators have been studied intensively in the last two decades. On the other hand these manipulators face with the trouble of having relatively smaller and limited workspace and difficulties in design and control. Therefore, parallel manipulators have become in the center of attention in various research areas.

There are many kinds of industrial robots which the end-effector moves along a contact surface in order to perform operations such as assembling, welding, grinding and deburring. In such applications, it is required to control the contact forces and motion along the specified directions on the contact surface.

Besides, manipulators exhibit joint drive flexibility behavior, and it is significant to take this into account in manipulator dynamics and control system design in order to obtain high precision systems. Rivin [1] showed experimentally that joint flexibility is the major source contributing to overall

robot flexibility. Also, Good et al. [2] showed that ignoring joint flexibility in manipulator dynamics and controller design causes degradation in performance of robots. Moreover, in some cases, joint flexibility may be a desired phenomenon in especially high load systems for structural reasons.

Spong [3] introduced a flexible joint model which has led to many researchers to study on flexible joint manipulators. He considered two nonlinear control schemes; inverse dynamics approach and singular perturbation approach. Inverse dynamics approach is based on elimination of intermediate variables analytically and to obtain input torques as functions of end-effector motion. The singular perturbation approach decomposes the system into slow (rigid manipulator) and fast (flexible joints) subsystems consequently, system order reduction is obtained.

Forrest-Barlach and Babcock [4] developed an inverse dynamics control structure for a rigid-link cylindrical coordinate arm with drive train compliance in the revolute and radial degree of freedom.

Jankowski and Van Brussel [5] presented inverse dynamics control in discrete-time. In order to avoid the problem of computational complexity which arises in classical inverse dynamics approach (resulting with the requirement of very high sampling rates), numerical solution of singular sets of differential equations is used.

Ider and Özgören [6] developed an inverse dynamics control algorithm at the acceleration level. Implicit numerical integration methods that account for the higher order derivative information are utilized for solving the singular set of differential equations. Joint and rotor positions and velocities are the feedback variables which are used to achieve asymptotic stability.

A hybrid force and motion trajectory control strategy for flexible joint robots is studied by Hu and Vukovich [7] based on the concept of singular perturbation.

Jankowski and Elmaraghy [8] presented an analytical inverse dynamics method for hybrid force and motion control. The input and output relationship is obtained by analytically eliminating the intermediate variables. The elimination procedure requires the differentiation of the equation of motion, the acceleration level constraint equations and task equations twice which adds complexity to calculations.

Ider [9] developed a force and motion trajectory control law for flexible joint robots by numerically solving the acceleration level dynamic equations which are singular. This study aims to avoid the drawbacks of classical methods.

Above mentioned studies are related on flexible joint serial manipulators. There are very few contributions in the literature about parallel manipulators which takes joint flexibility into account. Korkmaz [10] presented his M.S. thesis on trajectory tracking control of a flexible joint parallel manipulator by using the analytical inverse dynamics approach.

Survey of the literature related to modeling and control of flexible joint robots provided by Ozgoli and Taghirad [11] ,and Dwivedy and Eberhard [12].

1.2 Objective

This thesis aims at hybrid force and motion trajectory control of the end effector of a parallel manipulator, by using acceleration level analytical inverse dynamics approach while taking joint drive flexibility into consideration.

To facilitate the solution, acceleration level inverse dynamic equations which are singular are solved by using implicit numerical integration methods. Structural damping in actuated joints, viscous friction in unactuated joints and rotor damping characteristics are also included to the model. The control law proposed achieves simultaneous and asymptotically stable trajectory tracking control of the end-effector contact forces and the motion along the constraint

surfaces. It is aimed to avoid the further differentiations of the equation of motion, the constraint and task equations which cause complexity for calculations.

1.3 Outline of the Study

Following chapters are organized to explain the control method and the case study.

In Chapter 2, flexible joint model and the dynamics of a parallel manipulator with flexible joints are explained. Also, the system equation of motion and closed loop constraints are introduced.

In Chapter 3, inverse dynamics control approach is explained. Task space equations and the control law are introduced. The procedure to calculate the control torques using acceleration level inverse dynamics equations is explained. Also the procedure of elimination of unactuated joint variables from the system constraint equations is explained.

In Chapter 4, a case study is performed by applying the theoretical knowledge and method introduced in Chapters 2 & 3. A 2-RRR parallel manipulator is studied, and results of simulations performed via the inverse dynamics control method are presented.

Chapter 5 introduces a summary of the study, reviews and concludes the simulation results.

CHAPTER 2

MANIPULATOR DYNAMICS

2.1 Overview

Consider an *m*-link parallel manipulator with *n* actuator rotors connected by elastic transmissions. Usually, in a parallel manipulator the number of degree of freedom is as many as the number of joints actuated unless the system is overactuated or underactuated. Therefore, in this study it is taken as the parallel manipulator has *n* degree of freedom. The closed loop system can be converted into an open-tree structure by disconnecting a sufficient number of unactuated joints. The degree of freedom of the open-tree structure is *m*, where the number of independent loop closure equations is *m-n*. Let the set of generalized coordinates corresponding to manipulator joint variables be denoted as

$$G_1 = \{\theta_1, \dots, \theta_m\} \tag{2.1}$$

Therefore, manipulator joint variables of the open-tree system is denoted by the vector

$$\boldsymbol{\theta} = [\theta_1, \dots, \theta_m]^T \tag{2.2}$$

Let the manipulator joint variables be ordered such that the actuated and unactuated joint variables are divided into two subvectors as

$$\boldsymbol{\theta} = [\ \mathbf{q} \quad \boldsymbol{\theta}^{\mathbf{u}}]^T \tag{2.3}$$

where $\mathbf{q}$ is *n* x 1 vector of the actuated joint variables and $\boldsymbol{\theta}^{\mathbf{u}}$ *(m-n)* x 1 vector of the unactuated joint variables.

Elasticity in the transmission elements causes flexibility at the actuated joints. The sources of elasticity are harmonic drives, couplings, and thin shafts used in drive trains.

Joint elasticity and structural damping of an actuated flexible joint is modeled as a torsional spring and a torsional damper. Figure 2.1 demonstrates the dynamic model of a flexible joint.

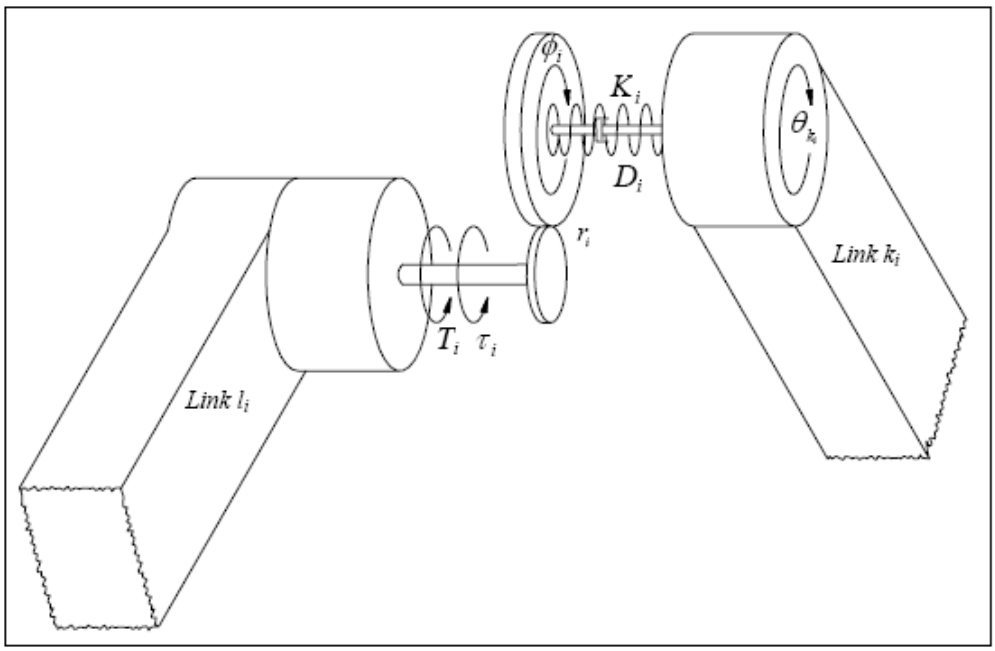

Figure 2.1 An Elastic Joint Model

The figure shows the i[th] transmission, where θ_{k_i} stands for manipulator joint variable which corresponds to angular position of the driven link (k_i) with respect to the link (l_i) that the i[th] actuator is mounted.

In this flexible joint model, τ_i stands for the rotor position of i[th] actuator with respect to the link that the actuator is mounted. ϕ_i, stands for the actuator variable which is obtained as

$$\phi_i = {}^{\tau_i}/_{r_i} \qquad i = 1, \dots, n \tag{2.4}$$

where r_i is the speed reduction ratio.

Second set of generalized coordinates corresponding to the actuator variables are

$$G_2 = \{\phi_1, \dots, \phi_n\} \tag{2.5}$$

Therefore, actuator joint variables of the manipulator is denoted by the vector

$$\boldsymbol{\phi} = [\phi_1, \dots, \phi_n]^T \tag{2.6}$$

For the i[th] transmission, K_i represents the spring constant and D_i represents the damping constant.

2.2 Manipulator Dynamics

Some assumptions which were stated by ref [3] are made in the modeling of the parallel manipulator in order to simplify the equations of motion and make them more appropriate for analysis and control.

- The gear ratio is large enough so that the kinetic energy of the rotor is due mainly to its own rotation. The rotational kinetic energy of the *i*th actuator is $1/2\left[I_i^r\left(\omega_z + r_i\dot{\phi}_i\right)^2 + I_i^{r*}\left(\omega_x^2 + \omega_y^2\right)\right]$ where I_i^r is the moment of inertia of the *i*th rotor about its rotational axis, I_i^{r*} is the moment of inertia of the cylindrical rotor about the axes perpendicular to the rotation axis through the mass center and $\omega_x, \omega_y, \omega_z$ are the angular velocity components of the link on which the actuator is mounted where the rotor angle is measured about z-axis. Since $\omega_x, \omega_y, \omega_z$ and $\dot{\phi}_i$ have the same order of magnitude, the rotational kinetic energy of the rotor is approximately $1/2\, I_i^r\left(r_i\dot{\phi}_i\right)^2$ if r_i is sufficiently large [13].

- The rotor/gear inertia is symmetric about the rotor axis of rotation so that the gravitational potential of the system and the velocity of the rotor center of mass are independent of rotor position.
- The links of the manipulator are rigid.

The elastic transmission between the links and the actuators introduce additional degrees of freedom. Therefore, rotor of each actuator is modeled as a fictitious link. As a result, *n* degree of freedom is added to the system which makes the overall system a *2n* degree of freedom system.

Lagrange's equations are used to find the equations of motion corresponding to two sets of generalized coordinates which were declared in Equations 2.1 and 2.5.

The Lagrange's equation for the first set of generalized coordinates corresponding to the manipulator joint variables

$$\frac{d}{dt}\left(\frac{\partial K}{\partial \dot{\theta}_j}\right) - \frac{\partial K}{\partial \theta_j} + \frac{\partial D}{\partial \dot{\theta}_j} + \frac{\partial U}{\partial \dot{\theta}_j} = \tilde{Q}_j + Q'_j \qquad j = 1, \dots, m \qquad (2.7)$$

The Lagrange's equation for the second set of generalized coordinates corresponding to the actuator joint variables

$$\frac{d}{dt}\left(\frac{\partial K}{\partial \dot{\phi}_i}\right) - \frac{\partial K}{\partial \phi_i} + \frac{\partial D}{\partial \dot{\phi}_i} + \frac{\partial U}{\partial \dot{\phi}_i} = Q''_i \qquad i = 1, \dots, n \qquad (2.8)$$

where *K*, *D*, *U*, $\tilde{Q}$, Q' and Q'' stand for kinetic energy, dissipation function, potential energy, generalized contact force, generalized constraint force and generalized actuator force terms respectively.

2.2.1 Kinetic Energy

Kinetic energy of a link can be defined as

$$KE_{Li} = \frac{1}{2} m_i^L \left(\bar{V}_{G_i}{}^L\right)^T \bar{V}_{G_i}{}^L + \frac{1}{2} (\bar{\omega}_i{}^L)^T \hat{I}_i{}^L \bar{\omega}_i{}^L \quad (2.9)$$

where

$$\bar{V}_{G_i}{}^L = \sum_{j=1}^{m} \bar{W}_{ij}^L \dot{\theta}_j \quad (2.10)$$

$$\bar{\omega}_i{}^L = \sum_{j=1}^{m} \bar{\Omega}_{ij}^L \dot{\theta}_j \quad (2.11)$$

$$\hat{I}_i{}^L = \left[\hat{C}^{(0,i)}\right] \underline{\hat{I}}_i^L \left[\hat{C}^{(0,i)}\right]^T \quad (2.12)$$

In the above equations,

m_i^L is the mass of the i[th] link.

$\bar{V}_{G_i}{}^L$ is the mass center velocity vector of the i[th] link as expressed in fixed reference frame.

$\bar{W}_{ij}^L$ is the velocity influence coefficient vector.

$\bar{\omega}_i{}^L$ is the angular velocity of the i[th] link as expressed in fixed reference frame.

$\bar{\Omega}_{ij}^L$ is the angular velocity influence coefficient vector.

$\hat{I}_i{}^L$ is the moment of inertia matrix of the i[th] link as expressed in fixed reference frame.

$\hat{C}^{(0,i)}$ is the transformation matrix from the reference frame attached to the i[th] link to the fixed reference frame.

$\underline{\hat{I}}_i^L$ is the moment of inertia matrix of the i[th] link as expressed in its body reference frame.

The kinetic energy of a link can be rewritten by substituting the Equations 2.10 and 2.11 into Equation 2.09:

$$KE_{Li} = \sum_{j=1}^{m} \sum_{k=1}^{m} m_{jki}^L \dot{\theta}_j \dot{\theta}_k \quad (2.13)$$

where

$$m_{jki}^{L} = 0.5 m_i^{L} \left(\bar{W}_{ij}{}^{L}\right)^{T} \bar{W}_{ik}{}^{L} + \frac{1}{2} \left(\bar{\Omega}_{ij}{}^{L}\right)^{T} \hat{I}_i{}^{L} \bar{\Omega}_{ik}{}^{L} \tag{2.14}$$

Kinetic energy of an actuator can be expressed similarly as

$$KE_{Ai} = 0.5 m_i^{A} \left(\bar{V}_{G_i}{}^{A}\right)^{T} \bar{V}_{G_i}{}^{A} + \frac{1}{2} \left(\bar{\omega}_i{}^{A}\right)^{T} \hat{I}_i{}^{A} \bar{\omega}_i{}^{L} \tag{2.15}$$

where

$$\bar{V}_{G_i}{}^{A} = \sum_{j=1}^{m} \bar{W}_{ij}^{A} \dot{\theta}_j \tag{2.16}$$

$$\bar{\omega}_i{}^{A} = \sum_{j=1}^{m} \bar{\Omega}_{l_i j}^{L} \dot{\theta}_j + \hat{C}^{(0,l_i)} \bar{u}_i \dot{\tau}_i \tag{2.17}$$

$$\hat{I}_i{}^{A} = \left[\hat{C}^{(0,i)}\right] \hat{I}_i^{A} \left[\hat{C}^{(0,i)}\right]^{T} \tag{2.18}$$

m_i^A is the mass of the i[th] actuator rotor.

$\bar{V}_{G_i}{}^{A}$ is the mass center velocity vector of the i[th] actuator as expressed in fixed reference frame.

$\bar{W}_{ij}^{A}$ is the velocity influence coefficient vector.

$\bar{\omega}_i{}^{A}$ is the angular velocity of the i[th] actuator rotor as expressed in fixed reference frame.

$\bar{\Omega}_{li,j}^{L}$ is the angular velocity influence coefficient vector of the previous link.

$\hat{I}_i{}^{A}$ is the moment of inertia matrix of the i[th] actuator rotor as expressed in fixed reference frame.

$\hat{C}^{(0,l_i)}$ is the transformation matrix from the reference frame attached to the l_i^{th} actuator rotor to the fixed reference frame.

$\hat{I}_i^A$ is the moment of inertia matrix of the ith actuator rotor as expressed in its body reference frame.

$\hat{C}^{(0,i)}$ is the transformation matrix from the reference frame attached to the ith actuator rotor to the fixed reference frame.

$\bar{u}_i$ is the unit vector along rotation axis of the ith actuator rotor in the link frame on which the actuator is mounted.

Assumption-1 which was introduced in Section 2.1 is called up into the formulation and the angular velocity of the i^{th} rotor turns out to be as

$$\bar{\omega}_i{}^A = \hat{C}^{(0,l_i)}\bar{u}_i\dot{t}_i \tag{2.19}$$

Therefore kinetic energy of an actuator can be expressed in more compact form as

$$KE_{Ai} = \frac{1}{2}m_i^A\left(\bar{V}_{G_i}^A\right)^T\bar{V}_{G_i}^A + \frac{1}{2}I_i^A\dot{t}_i^2 \tag{2.20}$$

By Assumption-2 which is associated with the mass distribution of the rotor, symmetric mass distribution is assumed. From symmetry consideration, it is assumed that the coordinate axes are principal axes of the cylinder. Moreover, mass center velocity of the actuator rotor $\bar{V}_{G_i}{}^A$ does not depend on the rotor position since mass center velocity is the translational velocity of the fixed point at the l_i^{th} link.

Total kinetic energy of the system is expressed as the sum of kinetic energy of the links and actuators.

$$K = \sum_{i=1}^{m} KE_{Li} + \sum_{i=1}^{n} KE_{Ai} \tag{2.21}$$

2.2.2 Potential Energy

For a rigid link, potential energy is due to gravity only, and depends on the position of the link. This fact can be expressed as

$$PE_{Li} = -\bar{g}^T m_i^L \bar{r}_i^L \tag{2.22}$$

where

$\bar{g}^T$ is the gravitational acceleration vector

$\bar{r}_i^L$ is the mass center position of the link as expressed in the fixed reference frame.

For an actuator, potential energy is due to the combination of both gravity and elastic potential of the joints. This is expressed as

$$PE_{Ai} = -\bar{g}^T m_i^A \bar{r}_i^A + \frac{1}{2} K_i \left(\theta_{k_i} - \phi_i\right)^2 \tag{2.23}$$

where

K_i is the spring constant of the joint of i^{th} transmission.

$\bar{r}_i^L$ is the mass center position of the actuator as expressed in the fixed reference frame.

Total potential energy of the system is expressed as the sum of potential energy of the links and actuators as expressed below.

$$U = \sum_{i=1}^{m} PE_{Li} + \sum_{i=1}^{n} PE_{Ai} \tag{2.24}$$

2.2.3 Dissipation Function

There is a positive definite dissipation function in the manipulator system which can be partitioned into four as

The dissipation function;

- due to structural damping at the actuated joints
- due to damping that occurs at the rotors of the actuators
- due to viscous friction at the unactuated joints
- due to viscous friction at the disconnected joints

Consequently, the total dissipative force of the manipulator is the sum of these individual dissipative forces.

Dissipation function due to structural damping at the actuated joints,

$$D^{\boldsymbol{a}} = \frac{1}{2}\sum_{i=1}^{n} D_i^a \left(\dot{\theta}_{k_i} - \dot{\phi}_i\right)^2 \tag{2.25}$$

where

D_i^a is the joint damping constant of ith transmission.

Dissipation function due to damping that occurs at the rotors of the actuators,

$$D^{\boldsymbol{r}} = \frac{1}{2}\sum_{i=1}^{n} D_i^r \left(r_i\dot{\phi}_i\right)^2 \tag{2.26}$$

where

D_i^r is the damping constant of ith actuator.

Dissipation function due to viscous friction at the unactuated joints,

$$D^u = \frac{1}{2}\sum_{i=1}^{m-n} D_i^u \, \dot{\theta}_{l_i}^2 \tag{2.27}$$

where

D_i^u is the joint damping constant of i[th] unactuated joint.

Finally, let D^d denote the dissipation function due to viscous friction at the disconnected joints.

Therefore, total dissipation forces of the system can be expressed as

$$D = D^a + D^r + D^u + D^d \tag{2.28}$$

2.2.4 Generalized Contact, Constraint and Actuator Forces

Generalized forces of the system model consist of generalized contact forces, generalized constraint forces and the forces inherent in the structural members of the drive trains. Contact forces are provided by drive trains and constraint forces are imposed on the system by disconnecting a sufficient number of unactuated joints.

The virtual work done by the manipulator corresponding to the first set of generalized coordinates, i.e. the manipulator variables is used to obtain the generalized contact forces. The virtual work done by the second set of generalized coordinates, i.e. the actuator variables is used to obtain the torques after speed reduction. Equations 2.29 & 2.30 indicate the virtual work done by

the manipulator corresponding to the manipulator and actuator variables respectively.

$$\delta\widetilde{W}_i = F_i^C \delta\theta_i \qquad i = 1, \dots m \tag{2.29}$$

$$\delta W''_{i+m} = T_i \delta\phi_i \qquad i = 1, \dots n \tag{2.30}$$

Therefore the generalized force terms obtained from the virtual work equations are found as

$$\tilde{Q}_i = F_i^C \qquad i = 1, \dots m \tag{2.31}$$

$$Q''_i = T_i \qquad i = 1, \dots n \tag{2.32}$$

m-n loop closure constraint equations are obtained by reconnecting the disconnected joints. This can be expressed at position level as

$$\psi_i(\theta_1, \dots, \theta_m) = 0 \qquad i = 1, .. (m-n) \tag{2.33}$$

Differentiating Equation 2.33, following velocity level relation is obtained,

$$\sum_{j=1}^{m} B_{ij}\, \dot{\theta}_j = 0 \qquad i = 1, .. (m-n) \tag{2.34}$$

which can be expressed in matrix form as

$$\mathbf{B\theta} = \mathbf{0} \tag{2.35}$$

where **B** is the $(m-n)$ x m constraint Jacobian matrix with

$$B_{ij} = {\partial \psi_i}/{\partial \theta_j} \tag{2.36}$$

Velocity level constraint equations can be written in virtual form in order to obtain generalized constraint forces.

$$\sum_{j=1}^{m} B_{ij}\,\delta\theta_j = 0 \qquad i = 1, \dots, (m-n) \tag{2.37}$$

Furthermore, it can be written as

$$\sum_{i=1}^{m-n} \mu_i \left[\sum_{j=1}^{m} B_{ij}\,\delta\theta_j \right] = 0 \tag{2.38}$$

$$\sum_{j=1}^{m} \left[\sum_{i=1}^{m-n} \mu_i B_{ij} \right] \delta\theta_j = 0 \tag{2.39}$$

Therefore, the generalized constraint forces corresponding to the manipulator variables can be defined as

$$Q_j^{'} = \sum_{i=1}^{m-n} \mu_i B_{ij} \qquad j = 1, \dots, m \tag{2.40}$$

where

μ_i are the Lagrange multipliers with $i = 1, \dots, m-n$

2.3 System Equations of Motion

Two sets of generalized coordinates lead to two sets of equations of motion for the dynamic system. When the kinetic energy, potential energy, dissipation forces and generalized forces which were described in previous sections, are imposed into Equations 2.7 and 2.8, and manipulated for both sets, equations of motion are obtained.

The equations of motion corresponding to the first set of generalized coordinates, i.e. the manipulator variables are

$$\sum_{k=1}^{n} M_{ik}^{L}\,\ddot{\theta}_i + Q_i + Da_i + St_i(\theta_i - \phi_i) - F_i^C - \sum_{i=1}^{m-n} \mu_i B_{ij} = 0 \qquad (2.41)$$

The equations of motion corresponding to the second set of generalized coordinates, i.e. the actuator variables are

$$I_i^r r_i^2 \ddot{\phi}_i + D_i^r r_i^2 \dot{\phi}_i - D_i\left(\dot{\theta}_i - \dot{\phi}_i\right) - K_i(\theta_i - \phi_i) = T_i \qquad (2.42)$$

The equations 2.41 and 2.42 can be written in matrix form as follows.

$$\mathbf{M}(\boldsymbol{\theta})\ddot{\boldsymbol{\theta}} + \mathbf{Q}\left(\boldsymbol{\theta}, \dot{\boldsymbol{\theta}}\right) + \mathbf{Da}\left(\dot{\boldsymbol{\theta}}, \dot{\boldsymbol{\phi}}\right) + \mathbf{St}(\boldsymbol{\theta}, \boldsymbol{\phi}) - \mathbf{F^C} - \mathbf{B^T}(\boldsymbol{\theta})\boldsymbol{\mu} = \mathbf{0} \qquad (2.43)$$

where

$\mathbf{M}(\boldsymbol{\theta})$ is the $m \times m$ symmetric positive definite generalized mass matrix,

$\mathbf{Q}\left(\boldsymbol{\theta}, \dot{\boldsymbol{\theta}}\right)$ is the $m \times 1$ vector which contains Coriolis, centrifugal and gravitational terms.

$\mathbf{Da}(\dot{\boldsymbol{\theta}}, \dot{\boldsymbol{\phi}})$ is the $m \times 1$vector which contains damping terms,

$\mathbf{St}(\boldsymbol{\theta}, \boldsymbol{\phi})$ is the $m \times 1$vector which contains stiffness terms,

$\mathbf{F^C}$ is the generalized contact force vector

$\mathbf{B^T(\theta)\mu}$ is the generalized constraint force vector

$\boldsymbol{\mu}$ is the $(m-n)\times 1$ vector whose elements consist of the Lagrange multipliers which mean the constraint forces imposed on the disconnected joint.

$$\mathbf{I^r}\ddot{\boldsymbol{\phi}} + \mathbf{D^r}\dot{\boldsymbol{\phi}} - \mathbf{D^a}\left(\dot{\mathbf{q}} - \dot{\boldsymbol{\phi}}\right) - \mathbf{K}(\mathbf{q} - \boldsymbol{\phi}) = \mathbf{T} \tag{2.44}$$

where

$\mathbf{I^r}$ is an $n \times n$ matrix whose elements are the inertial parameters of the links and can be expressed as

$$\mathbf{I^r} = diag[I_i^r r_i^2] \tag{2.45}$$

$\mathbf{D^r}$ is an $n\times n$ matrix whose elements are the inertial parameters of the rotors and can be expressed as

$$\mathbf{D^r} = diag[D_i^r r_i^2] \tag{2.46}$$

$\mathbf{D^a}$ is an $n\times n$ matrix whose elements are damping constants of the actuated joints and can be expressed as

$$\mathbf{D^a} = diag[D_i] \tag{2.47}$$

$\mathbf{K}$ is an $n\times n$ matrix whose elements are spring constants of the actuated joints and can be expressed as

$$\mathbf{K} = diag[K_i] \tag{2.48}$$

$\mathbf{T}$ is an $n\times 1$ vector whose elements are control torques after speed reduction.

2.4 Constraint Equations

System constraint equations are essential for derivation of generalized forces as mentioned in Section 2.2.4.

Let the Cartesian end-effector coordinates be represented as x_i, i=1..,n. The relation between the end-effector Cartesian coordinates and the generalized coordinates, i.e the joint variables θ_m can be expressed as

$$\mathbf{x} = f(\boldsymbol{\theta}) \tag{2.49}$$

The contact of the manipulator end-effector with the environment can be described by following constraint equations.

$$g_i(x,t) = 0 \qquad i=1,\ldots,r \tag{2.50}$$

Above equation can be written in velocity level and writing x and $\dot{x}$ in terms of θ and $\dot{\theta}$ as follows

$$E_{ij}(\theta,t)\dot{\theta}_j + G_i(\theta,t) = 0 \qquad i=1,\ldots,r \tag{2.51}$$

where

$$E_{ij} = {\partial g_i}\Big/{\partial \dot{\theta}_j} \tag{2.52}$$

Equation can be written in matrix form as

$$\mathbf{E}\dot{\boldsymbol{\theta}} + \mathbf{G} = \mathbf{0} \tag{2.53}$$

where **E** is an $r \times m$ matrix.

Generalized contact forces can be expressed as

$$\mathbf{F^c} = \mathbf{E^T}\lambda \tag{2.54}$$

where

λ is the vector of Lagrange multipliers that represent the contact forces which are perpendicular to the constraint surface

Also, *m-n* constraint equations are derived by disconnecting sufficient number of unactuated joints which are necessary to obtain generalized constraint forces. This physically means the net torque applied by the joint forces at the disconnected joint(s). Constraint equations are also used to express unactuated joint coordinates in terms of the actuated ones which are necessary to reduce the number of dynamic equations by eliminating the unactuated joint variables.

As described in Section 2.1, manipulator joint variables can be partitioned into two subvectors as

$$\dot{\boldsymbol{\theta}} = \begin{bmatrix} \dot{\mathbf{q}} & \dot{\boldsymbol{\theta}}^{\mathbf{u}} \end{bmatrix}^T \tag{2.55}$$

where $\dot{\mathbf{q}}$ is *n* x 1 vector of the actuated joint variables and $\dot{\boldsymbol{\theta}}^{\mathbf{u}}$ *(m-n)* x 1 vector of the unactuated joint variables.

Loop closure equations are used to construct *(m-n)* × *m* matrix **B** as in Equation 2.34. Matrix **B** can be subdivided into two subvectors as

$$\mathbf{B} = [\mathbf{B}^{\mathbf{a}} \quad \mathbf{B}^{\mathbf{u}}] \tag{2.56}$$

where $\mathbf{B}^{\mathbf{a}}$ is an *(m-n)* × *n* matrix corresponding to actuated joint variables and $\mathbf{B}^{\mathbf{u}}$ is an *(m-n)* × *(m-n)* matrix corresponding to unactuated joint variables

ence Equation 2.35 can be written as

$$\mathbf{B}^{\mathbf{u}}\dot{\boldsymbol{\theta}}^{\mathbf{u}} = -\mathbf{B}^{\mathbf{a}}\dot{\mathbf{q}} \tag{2.57}$$

Above equation can be solved for $\boldsymbol{\theta}^{\mathbf{u}}$ as follows.

$$\dot{\boldsymbol{\theta}}^{\mathbf{u}} = -(\mathbf{B}^{\mathbf{u}})^{-1}\mathbf{B}^{\mathbf{a}}\dot{\mathbf{q}} \tag{2.58}$$

Further differentiation of the Equation 2.58 yields

$$\ddot{\boldsymbol{\theta}}^{\mathbf{u}} = -\left(\left(\dot{\mathbf{B}}^{\mathbf{u}}\right)^{-1}\mathbf{B}^{\mathbf{a}} + (\mathbf{B}^{\mathbf{u}})^{-1}\dot{\mathbf{B}}^{\mathbf{a}}\right)\dot{\mathbf{q}} - (\mathbf{B}^{\mathbf{u}})^{-1}\mathbf{B}^{\mathbf{a}}\ddot{\mathbf{q}} \tag{2.59}$$

CHAPTER 3

INVERSE DYNAMICS CONTROL

3.1 Task Space Equations

The control method used for the parallel manipulator is based on the calculation of input torques in order the system to perform the specified tasks. The prescribed end-effector contact forces and the prescribed motion trajectories along the constraint surfaces are the tasks of the manipulator.

It is necessary to specify a relation between input and outputs of the system. System inputs are joint torques, or voltages applied to the actuators and system outputs are the end-effector contact force and independent end-effector positions along the constraint surfaces.

Let the independent coordinates along the constraint surface represented as y_i, i=1..,n - r which can be expressed as

$$y_i = h_i(x,t) \qquad i = 1,\dots,(n-r) \tag{3.1}$$

Above expression leads to the following velocity relation with writing x and $\dot{x}$ in terms of θ and $\dot{\theta}$

$$\dot{y}_i = \sum_{j=1}^{n} P_{ij}(\theta,t)\dot{\theta}_j + H_i(\theta,t) \qquad i = 1,\dots,(n-r) \tag{3.2}$$

where

$$P_{ij} = {\partial h_i}/{\partial \dot{\theta}_j} \tag{3.3}$$

Equation 3.2 can be written in matrix form as

$$\mathbf{y} = \mathbf{P}\dot{\boldsymbol{\theta}} + \mathbf{H} \tag{3.4}$$

where **P** is the *(n-r)* × *m* manipulator Jacobian matrix.

The matrices **E** and **P** which were derived in Equations 2.52 and 3.3 respectively can be written in terms of actuated variables, by making use of the Equation 2.58.

E can be partitioned into *r* × *n* matrix $\mathbf{E^a}$ and *r* × *(m-n)* matrix $\mathbf{E^u}$ according to the the coefficient matrices of the joint variables to which they correspond. This can be expressed as follows.

$$[\mathbf{E^a} \quad \mathbf{E^u}] \begin{bmatrix} \dot{\mathbf{q}} \\ \dot{\boldsymbol{\theta}}^{\mathbf{u}} \end{bmatrix} + \mathbf{G} = \mathbf{0} \tag{3.5}$$

Above equation can be written as

$$\mathbf{E^a}\dot{\mathbf{q}} + \mathbf{E^u}\dot{\boldsymbol{\theta}}^{\mathbf{u}} + \mathbf{G} = \mathbf{0} \tag{3.6}$$

Substituting Equation 2.58 into Equation 3.6 yields

$$\mathbf{E^a}\dot{\mathbf{q}} + \mathbf{E^u}[-(\mathbf{B^u})^{-1}\mathbf{B^a}\dot{\mathbf{q}}] + \mathbf{G} = \mathbf{0} \tag{3.7}$$

Factoring out the joint coordinates of the actuated variables yields

$$\mathbf{E}^*\dot{\mathbf{q}} + \mathbf{G} = \mathbf{0} \tag{3.8}$$

where $\mathbf{E}^*$ is *r* × *n* matrix as below.

$$\mathbf{E}^* = \mathbf{E^a} - \mathbf{E^u}(\mathbf{B^u})^{-1}\mathbf{B^a} \tag{3.9}$$

Differentiating Equation 3.8 gives

$$\mathbf{E}^{*}\ddot{\mathbf{q}} + \dot{\mathbf{E}}^{*}\dot{\mathbf{q}} + \dot{\mathbf{G}} = \mathbf{0} \tag{3.10}$$

Similar operations can be performed for partition of **P** and following expression can be obtained.

$$\mathbf{P}^{*}\dot{\mathbf{q}} + \mathbf{H} = \dot{\mathbf{y}} \tag{3.11}$$

where $\mathbf{P}^{*}$ is *(n-r)* × *n* matrix as below.

$$\mathbf{P}^{*} = \mathbf{P}^{\mathbf{a}} - \mathbf{P}^{\mathbf{u}}(\mathbf{B}^{\mathbf{u}})^{-\mathbf{1}}\mathbf{B}^{\mathbf{a}} \tag{3.12}$$

Differentiating Equation 3.11 gives

$$\mathbf{P}^{*}\ddot{\mathbf{q}} + \dot{\mathbf{P}}^{*}\dot{\mathbf{q}} + \dot{\mathbf{H}} = \ddot{\boldsymbol{y}} \tag{3.13}$$

Equations 3.8 and 3.11 can be written in augmented form as follows.

$$\begin{bmatrix}\mathbf{E}^{*}\\ \mathbf{P}^{*}\end{bmatrix}\dot{\mathbf{q}} + \begin{bmatrix}\mathbf{G}\\ \mathbf{H}\end{bmatrix} = \begin{bmatrix}\mathbf{0}\\ \dot{\mathbf{y}}\end{bmatrix} \tag{3.14}$$

Therefore, the relation between the actuated joint coordinates and the independent end-effector coordinates can be defined as

$$\dot{\mathbf{q}} = \boldsymbol{\nu}\dot{\mathbf{y}} - (\boldsymbol{\eta}\mathbf{G} + \boldsymbol{\nu}\mathbf{H}) \tag{3.15}$$

where *n x m* matrix $\boldsymbol{\eta}$ and *n x (n-m)* matrix $\boldsymbol{\nu}$ are defined as

$$[\boldsymbol{\eta} \quad \boldsymbol{\nu}] = \begin{bmatrix}\mathbf{E}^{*}\\ \mathbf{P}^{*}\end{bmatrix}^{-\mathbf{1}} \tag{3.16}$$

At this point, it is convenient to write the system equations of motion in terms of the actuated joint variables by eliminating the unactuated joint accelerations and the Lagrange multipliers μ which represent the forces at the disconnected joints.

M and **Q** can be partitioned according to the actuated and unactuated joint variables to which they correspond as follows.

$$\mathbf{M} = \begin{bmatrix} \mathbf{M^{aa}} & \mathbf{M^{au}} \\ \mathbf{M^{au^T}} & \mathbf{M^{uu}} \end{bmatrix} \tag{3.17}$$

and

$$\mathbf{Q} = \begin{bmatrix} \mathbf{Q^a} \\ \mathbf{Q^u} \end{bmatrix} \tag{3.18}$$

where

$\mathbf{M^{aa}}$ is an $n \times n$ submatrix generated from symmetric generalized mass matrix.

$\mathbf{M^{au}}$ is an $n \times (m\text{-}n)$ submatrix generated from symmetric generalized mass matrix.

$\mathbf{M^{uu}}$ is an $(m\text{-}n) \times (m\text{-}n)$ submatrix generated from symmetric generalized mass matrix.

$\mathbf{Q^a}$ is an $n \times 1$ submatrix generated from $\mathbf{Q}$ vector that contains centrifugal, Coriolis and gravitational terms

$\mathbf{Q^u}$ is an $(m\text{-}n) \times 1$ submatrix generated from $\mathbf{Q}$ vector that contains centrifugal, Coriolis and gravitational terms

Equation 2.43 can be written in two parts as

$$\mathbf{M^{aa}\ddot{q} + M^{au}\ddot{\theta}^u + Q^a + D^a(\dot{q} - \dot{\phi}) + K(q - \phi) + E^*\lambda - B^{a^T}\mu = 0} \tag{3.19}$$

and

$$\mathbf{M^{au^T}\ddot{q} + M^{uu}\ddot{\theta}^u + Q^u + R\dot{\theta}^u - B^{u^T}\mu = 0} \tag{3.20}$$

where

$\mathbf{R}$ is an $(m\text{-}n) \times (m\text{-}n)$ matrix containing the dissipation terms related to the unactuated joints.

Equation 3.20 can be solved for Lagrange multipliers as follows.

$$\boldsymbol{\mu} = \left(\mathbf{B}^{\mathbf{u}^{\mathbf{T}}}\right)^{-1}\left\{\mathbf{M}^{\mathbf{au}^{\mathbf{T}}}\ddot{\mathbf{q}} + \mathbf{M}^{\mathbf{uu}}\ddot{\boldsymbol{\theta}}^{\mathbf{u}} + \mathbf{Q}^{\mathbf{u}} + \mathbf{R}\dot{\boldsymbol{\theta}}^{\mathbf{u}}\right\} \tag{3.21}$$

Substituting Equations 2.58, 2.59 and Equation 3.21 into Equation 3.19 yields the *n* dimensional dynamic equation shown below.

$$\mathbf{M}^{*}\ddot{\mathbf{q}} + \mathbf{Q}^{*} + \mathbf{D}^{\mathbf{a}}\left(\dot{\mathbf{q}} - \dot{\boldsymbol{\phi}}\right) + \mathbf{K}(\mathbf{q} - \boldsymbol{\phi}) + \mathbf{E}^{*}\boldsymbol{\lambda} = \mathbf{0} \tag{3.22}$$

where,

$$\mathbf{M}^{*} = \left[\mathbf{M}^{\mathbf{aa}} - \mathbf{M}^{\mathbf{au}}\mathbf{B}^{\mathbf{u}-\mathbf{1}}\mathbf{B}^{\mathbf{a}}\right] - \mathbf{B}^{\mathbf{a}^{\mathbf{T}}}\left(\mathbf{B}^{\mathbf{u}-\mathbf{1}}\right)^{\mathbf{T}}\left[\mathbf{M}^{\mathbf{au}^{\mathbf{T}}} - \mathbf{M}^{\mathbf{uu}}\mathbf{B}^{\mathbf{u}-\mathbf{1}}\mathbf{B}^{\mathbf{a}}\right] \tag{3.23}$$

$$\begin{aligned}\mathbf{Q}^{*} = {} & \left[-\mathbf{M}^{\mathbf{au}}\mathbf{B}^{\mathbf{u}-\mathbf{1}}\dot{\mathbf{B}}^{\mathbf{a}} + \mathbf{B}^{\mathbf{a}^{\mathbf{T}}}\left(\mathbf{B}^{\mathbf{u}-\mathbf{1}}\right)^{\mathbf{T}}\mathbf{M}^{\mathbf{uu}}\mathbf{B}^{\mathbf{u}-\mathbf{1}}\dot{\mathbf{B}}^{\mathbf{a}}\right]\dot{\mathbf{q}} \\ & + \left[-\mathbf{M}^{\mathbf{au}}\mathbf{B}^{\mathbf{u}-\mathbf{1}}\dot{\mathbf{B}}^{\mathbf{u}} + \mathbf{B}^{\mathbf{a}^{\mathbf{T}}}\left(\mathbf{B}^{\mathbf{u}-\mathbf{1}}\right)^{\mathbf{T}}\mathbf{M}^{\mathbf{uu}}\mathbf{B}^{\mathbf{u}-\mathbf{1}}\dot{\mathbf{B}}^{\mathbf{u}} + \mathbf{R}\right]\dot{\boldsymbol{\theta}}^{\mathbf{u}} + \mathbf{Q}^{\mathbf{a}} \\ & - \mathbf{B}^{\mathbf{a}^{\mathbf{T}}}\left(\mathbf{B}^{\mathbf{u}-\mathbf{1}}\right)^{\mathbf{T}}\mathbf{Q}^{\mathbf{u}}\end{aligned} \tag{3.24}$$

Intermediate variables **q** and **Φ** can be eliminated from the dynamic equations to obtain a relation between the input torque **T** and outputs which are the contact forces λ and independent coordinates of end effector along constraint surface, **y**. After the similar elimination procedure which is explained in ref [1], the input output relation is obtained as follows.

$$\mathbf{A}(\mathbf{y})\mathbf{y}^{(\mathbf{4})} + \mathbf{Z}(\mathbf{y})\ddot{\boldsymbol{\lambda}} + \mathbf{R}\left(\dddot{\mathbf{y}}, \ddot{\mathbf{y}}, \dot{\mathbf{y}}, \mathbf{y}, \dot{\boldsymbol{\lambda}}, \boldsymbol{\lambda}\right) = \mathbf{T} + \mathbf{S}\dot{\mathbf{T}} \tag{3.25}$$

where

$$\mathbf{A} = \mathbf{K}^{-\mathbf{1}}\mathbf{I}^{\mathbf{R}}\mathbf{M}^{*}\boldsymbol{\nu} \tag{3.26}$$

$$\mathbf{Z} = \mathbf{K^{-1}I^{r}E^{*T}} \tag{3.27}$$

$$\mathbf{S} = \mathbf{K^{-1}D} \tag{3.28}$$

$$\begin{aligned}\mathbf{R} = \mathbf{K^{-1}}\Big\{\mathbf{I^{r}}\Big[\mathbf{M^{*}}\Big(&\mathbf{3\dot{\nu}\ddot{\gamma} + 3\ddot{\nu}\dot{\gamma} + \dddot{\nu}\gamma} \\ &\mathbf{- \big(\ddot{\eta}G + 3\ddot{\eta}\dot{G} + 3\dot{\eta}\ddot{G} + \eta\dddot{G} + \dddot{\nu}H + 3\ddot{\nu}\dot{H} + 3\dot{\nu}\ddot{H} + \eta\dddot{H}\big)} \\ &\mathbf{+ 2\dot{M}^{*}\ddot{q} + \ddot{M}\dot{q} + \dddot{Q}^{*} + D\dddot{q} + K\ddot{q} + \ddot{E}^{*T}\lambda + E^{*T}\dddot{\lambda}}\Big)\Big] \\ &\mathbf{+ D^{r}(D\ddot{q} + K\dot{q})} \\ &\mathbf{+ (D + D^{r})\Big(M^{*}\ddot{q} + \dot{M}^{*}\dot{q} + \ddot{Q}^{*} + \dot{E}^{*T}\lambda + E^{*T}\ddot{\lambda}\Big)\Big\} + M^{*}\ddot{q} + Q^{*}} \\ &\mathbf{+ E^{*T}\lambda}\end{aligned} \tag{3.29}$$

An inverse dynamics control law can be formulated using the above equation which will linearize and decouple the system. Corresponding control torque vector **T** can be calculated by using numerical integration. However, this operation will require the calculation of $\ddot{\mathbf{M}}, \dot{\mathbf{M}}, \ddot{\mathbf{Q}}, \dot{\mathbf{Q}}, \ddot{\eta}, \dddot{\eta}, \ddot{\nu}, \dddot{\nu}, \ddot{G}, \dddot{G}, \ddot{H}, \dddot{H}$ which will cause extremely long and complex expressions which will end up with long computation time. As a result, this approach is impractical for real time applications especially for systems with degrees of freedom more than 3 [9].

3.2 Control Law

In order to avoid the drawbacks of the above mentioned algorithm, the dynamic equations will be utilized at the acceleration level to compute the required input torques.

Equations 3.22, 2.42, 3.10 and 3.13 can be written in augmented form as below.

$$\begin{bmatrix} \mathbf{M}^* & \mathbf{0} & \mathbf{0} \\ \mathbf{0} & \mathbf{I}^r & \mathbf{I} \\ \mathbf{E}^* & \mathbf{0} & \mathbf{0} \\ \mathbf{P}^* & \mathbf{0} & \mathbf{0} \end{bmatrix} \begin{bmatrix} \ddot{\mathbf{q}} \\ \ddot{\boldsymbol{\phi}} \\ \mathbf{T} \end{bmatrix} = \begin{bmatrix} -\mathbf{Q}^* - \mathbf{D}(\dot{\mathbf{q}} - \dot{\boldsymbol{\phi}}) - \mathbf{K}(\mathbf{q} - \boldsymbol{\phi}) - \mathbf{E}^{*\mathbf{T}}\Gamma \\ \mathbf{D}(\dot{\mathbf{q}} - \dot{\boldsymbol{\phi}}) + \mathbf{K}(\mathbf{q} - \boldsymbol{\phi}) \\ -\dot{\mathbf{E}}^*\dot{\mathbf{q}} - \dot{\mathbf{G}} \\ -\dot{\mathbf{P}}^*\dot{\mathbf{q}} - \dot{\mathbf{H}} + \mathbf{z} \end{bmatrix} \tag{3.30}$$

$\ddot{\boldsymbol{y}}$ and λ are replaced by control variables **z** and Γ which represent 'command accelerations' and 'command contact forces' respectively.

Equation 3.25 shows that, in the forward dynamics, torque vector **T** instantaneously affects the end-effector jerk rate $y^{(4)}$ and end-effector contact force second derivative $\ddot{\lambda}$. In order to linearize and decouple the system, highest order derivative in the input output relation should be taken into consideration, therefore in the control law command jerk rates and command contact force second derivatives should be expressed. $\dddot{z}$ and $\ddot{\Gamma}$ can be formulated with errors and the desired values which are denoted by superscript *d* as below.

$$\ddot{\mathbf{z}} = \mathbf{y}^{(\mathbf{4})\mathbf{d}} + \mathbf{C_1}\left(\mathbf{y}^{(\mathbf{3})\mathbf{d}} - \mathbf{y}^{(\mathbf{3})}\right) + \mathbf{C_2}\left(\ddot{\mathbf{y}}^{\mathbf{d}} - \ddot{\mathbf{y}}\right) + \mathbf{C_3}\left(\ddot{\mathbf{y}}^{\mathbf{d}} - \ddot{\mathbf{y}}\right) + \mathbf{C_4}\left(\ddot{\mathbf{y}}^{\mathbf{d}} - \ddot{\mathbf{y}}\right) \tag{3.31}$$

and

$$\ddot{\Gamma} = \ddot{\lambda}^{\mathrm{d}} + \mathbf{B_1}\left(\dot{\lambda}^{\mathrm{d}} - \dot{\lambda}\right) + \mathbf{B_2}(\lambda^{\mathrm{d}} - \lambda) \tag{3.32}$$

where $\mathbf{C_i}$, and $\mathbf{B_i}$ are constant feedback diagonal matrices which can be formulated as below.

$$\mathbf{C_i} = diag\left[C_{ij}\right] \qquad i = 1, \dots 4 \qquad j = 1, \dots, n - r \tag{3.33}$$

$$\mathbf{B_i} = diag\left[B_{ij}\right] \qquad i = 1, 2 \qquad j = 1, \dots, r \tag{3.34}$$

For the inverse dynamics problem solution, Equation 3.30 can be written with rows that involve only kinematic variables. First, third and fourth rows of the Equation 3.30 will yield the inverse kinematic equations. It involves inertia, elastic and prescribed contact force terms because of the joint flexibility in the system. Second row of the Equation 3.30 is for computing torques. Hence, inverse kinematic equations can be written as below.

$$\begin{bmatrix} \mathbf{M}^* & \mathbf{0} \\ \mathbf{E}^* & \mathbf{0} \\ \mathbf{P}^* & \mathbf{0} \end{bmatrix} \begin{bmatrix} \ddot{\mathbf{q}} \\ \ddot{\boldsymbol{\phi}} \end{bmatrix} = \begin{bmatrix} -\mathbf{Q}^* - \mathbf{D}(\dot{\mathbf{q}} - \dot{\boldsymbol{\phi}}) - \mathbf{K}(\mathbf{q} - \boldsymbol{\phi}) - \mathbf{E}^{*\mathbf{T}}\Gamma \\ -\dot{\mathbf{E}}^*\dot{\mathbf{q}} - \dot{\mathbf{G}} \\ -\dot{\mathbf{P}}^*\dot{\mathbf{q}} - \dot{\mathbf{H}} + \mathbf{z} \end{bmatrix} \tag{3.35}$$

However, acceleration coefficient matrix in Equation 3.35 is not invertible which leads to a singular set of differential equations. This is caused by the elastic media where the torques are transmitted to the end-effector. Elasticity in the joints prevent the control torques to have instantaneous effect on the end-effector accelerations and contact forces which can also be justified by Equation 3.25 showing the control torques have effect on second derivatives of end-effector accelerations and contact forces.

Since explicit system of ordinary differential equations cannot be obtained from Equation 3.35 because of the singularity, implicit numerical integration methods must be used. Among the implicit integration methods, backward Euler method will be applied.

Below shown backward difference approximation is used to obtain backward Euler formulation.

$$\dot{y}_{k+1} \approx (y_{k+1} - y_k)/h \tag{3.36}$$

Therefore, the backward Euler method is shown as

$$y_{k+1} = h\dot{y}_{k+1} + y_k \tag{3.37}$$

where h is the sampling time and k is the time step number.

At this point, Equation 3.30 can be rewritten by using Equation 3.37 at time t_{k+1}. To do this, $\ddot{\mathbf{q}}, \mathbf{q}, \ddot{\boldsymbol{\phi}}$ and $\boldsymbol{\phi}$ are replaced by $\frac{1}{h}(\dot{\mathbf{q}}_{\mathbf{k+1}} - \dot{\mathbf{q}}_{\mathbf{k}})$, $h\dot{\mathbf{q}}_{\mathbf{k+1}} + \mathbf{q}_{\mathbf{k}}$, $\frac{1}{h}(\dot{\boldsymbol{\phi}}_{\mathbf{k+1}} - \dot{\boldsymbol{\phi}}_{\mathbf{k}})$ and $h\dot{\boldsymbol{\phi}}_{\mathbf{k+1}} + \boldsymbol{\phi}_{\mathbf{k}}$ respectively as follows.

$$\mathbf{M}^* \frac{1}{h}(\dot{\mathbf{q}}_{\mathbf{k+1}} - \dot{\mathbf{q}}_{\mathbf{k}}) + \mathbf{Q}^* + \mathbf{D}^{\mathbf{a}}(\dot{\mathbf{q}}_{\mathbf{k+1}} - \dot{\boldsymbol{\phi}}_{\mathbf{k+1}}) + \mathbf{K}(h\dot{\mathbf{q}}_{\mathbf{k+1}} + \mathbf{q}_{\mathbf{k}} - h\dot{\boldsymbol{\phi}}_{\mathbf{k+1}} - \boldsymbol{\phi}_{\mathbf{k}}) + \mathbf{E}^{*\mathbf{T}}\boldsymbol{\Gamma}_{\mathbf{k+1}} = \mathbf{0} \tag{3.38}$$

$$\mathbf{I}^{\mathbf{r}} \frac{1}{h}(\dot{\boldsymbol{\phi}}_{\mathbf{k+1}} - \dot{\boldsymbol{\phi}}_{\mathbf{k}}) + \mathbf{D}^{\mathbf{r}}\dot{\boldsymbol{\phi}}_{\mathbf{k+1}} - \mathbf{D}(\dot{\mathbf{q}}_{\mathbf{k+1}} - \dot{\boldsymbol{\phi}}_{\mathbf{k+1}}) - \mathbf{K}(h\dot{\mathbf{q}}_{\mathbf{k+1}} + \mathbf{q}_{\mathbf{k}} - h\dot{\boldsymbol{\phi}}_{\mathbf{k+1}} - \boldsymbol{\phi}_{\mathbf{k}}) = \mathbf{T}_{\mathbf{k+1}} \tag{3.39}$$

$$\mathbf{E}^* \frac{1}{h}(\dot{\mathbf{q}}_{\mathbf{k+1}} - \dot{\mathbf{q}}_{\mathbf{k}}) + \dot{\mathbf{E}}^* \dot{\mathbf{q}}_{k+1} + \dot{\mathbf{G}} = \mathbf{0} \tag{3.40}$$

$$\mathbf{P}^* \frac{1}{h}(\dot{\mathbf{q}}_{\mathbf{k+1}} - \dot{\mathbf{q}}_{\mathbf{k}}) + \dot{\mathbf{P}}^* \dot{\mathbf{q}}_{k+1} + \dot{\mathbf{H}} = \mathbf{z}_{\mathbf{k+1}} \tag{3.41}$$

In the above equations $\mathbf{M}^*(h\dot{\mathbf{q}}_{\mathbf{k+1}} + \mathbf{q}_{\mathbf{k}})$, $\mathbf{Q}^*(h\dot{\mathbf{q}}_{\mathbf{k+1}} + \mathbf{q}_{\mathbf{k}}, \dot{\mathbf{q}}_{\mathbf{k+1}})$, $\mathbf{E}^*(h\dot{\mathbf{q}}_{\mathbf{k+1}} + \mathbf{q}_{\mathbf{k}}, t)$, $\dot{\mathbf{E}}^*(h\dot{\mathbf{q}}_{\mathbf{k+1}} + \mathbf{q}_{\mathbf{k}}, \dot{\mathbf{q}}_{\mathbf{k+1}}, t)$, $\mathbf{P}^*(h\dot{\mathbf{q}}_{\mathbf{k+1}} + \mathbf{q}_{\mathbf{k}}, t)$, $\dot{\mathbf{P}}^*(h\dot{\mathbf{q}}_{\mathbf{k+1}} + \mathbf{q}_{\mathbf{k}}, \dot{\mathbf{q}}_{\mathbf{k+1}}, t)$, $\dot{\mathbf{G}}(h\dot{\mathbf{q}}_{\mathbf{k+1}} + \mathbf{q}_{\mathbf{k}}, \dot{\mathbf{q}}_{\mathbf{k+1}}, t)$ and $\dot{\mathbf{H}}(h\dot{\mathbf{q}}_{\mathbf{k+1}} + \mathbf{q}_{\mathbf{k}}, \dot{\mathbf{q}}_{\mathbf{k+1}}, t)$ depend on $\dot{\mathbf{q}}_{\mathbf{k+1}}$. Equations 3.40 and 3.41 represent *n* number of nonlinear algebraic equations. Therefore, Equations 3.38 - 3.41 represent *3n* algebraic equations which can lead to the solution of *3n* unknowns which are $\dot{\mathbf{q}}_{\mathbf{k+1}}$, $\dot{\boldsymbol{\phi}}_{\mathbf{k+1}}$ and $\mathbf{T}_{\mathbf{k+1}}$.

For the calculation of unknowns, command accelerations $\mathbf{z}_{\mathbf{k+1}}$ and command contact forces $\boldsymbol{\Gamma}_{\mathbf{k+1}}$ need to be specified. Therefore it is required to integrate Equations 3.31 and 3.32 twice. Since desired motion and force trajectories are given as piecewise smooth functions in common practical applications, let the integration be performed in the time interval $t_a \leq t < t_b$.

Integration of Equation 3.31 twice yields the following expression.

$$\mathbf{z} = \mathbf{z_a} + \dot{\mathbf{z}}_\mathbf{a}(t - t_a) + \ddot{\mathbf{y}}^\mathbf{d} - \ddot{\mathbf{y}}_\mathbf{a}^\mathbf{d} - \dddot{\mathbf{y}}_\mathbf{a}^\mathbf{d}(t - t_a) + \mathbf{C_1}\left[\left(\dot{\mathbf{y}}^\mathbf{d} - \dot{\mathbf{y}}\right) - \left(\dot{\mathbf{y}}_\mathbf{a}^\mathbf{d} - \dot{\mathbf{y}}_\mathbf{a}\right) - \left(\ddot{\mathbf{y}}_\mathbf{a}^\mathbf{d} - \ddot{\mathbf{y}}_\mathbf{a}\right)(\mathbf{t} - \mathbf{t_a})\right] + \mathbf{C_2}\left[\left(\mathbf{y}^\mathbf{d} - \mathbf{y}\right) - \left(\mathbf{y}_\mathbf{a}^\mathbf{d} - \mathbf{y_a}\right) - \left(\dot{\mathbf{y}}_\mathbf{a}^\mathbf{d} - \dot{\mathbf{y}}_\mathbf{a}\right)(t - t_a)\right] - \mathbf{C_3}\left(\mathbf{y}_\mathbf{a}^\mathbf{d} - \mathbf{y_a}\right)(t - t_a) + \mathbf{C_3}\int_{\mathbf{t_a}}^{\mathbf{t}} \ddot{\mathbf{w}}(\tau)d\tau + \mathbf{C_4}\int_{\mathbf{t_a}}^{\mathbf{t}}\left[\int_{\mathbf{t_a}}^{\mathbf{t}} \ddot{\mathbf{w}}(s)ds\right]d\tau \tag{3.42}$$

where $\ddot{\mathbf{w}} = \mathbf{y}^\mathbf{d} - \mathbf{y}$.

And integration of Equation 3.32 twice yields the following expression.

$$\Gamma = \Gamma_a + \dot{\Gamma}_a(t - t_a) + \lambda^d - \lambda_a^d - \dot{\lambda}_a^d(t - t_a) - \mathbf{B_1}(\lambda_a^d - \lambda_a)(t - t_a) + \mathbf{B_1}\int_{t_a}^{t} \ddot{p}(\tau)d\tau + \mathbf{B_2}\int_{t_a}^{t}\left[\int_{t_a}^{t} \ddot{p}(s)ds\right]d\tau \tag{3.43}$$

where $\ddot{p} = \lambda^d - \lambda$.

Since the dynamic equations are written at time t_{k+1}, $\mathbf{z_{k+1}}$ and Γ_{k+1} are written in discrete time and use the $\mathbf{y}$, $\mathbf{y}^\mathbf{d}$, $\boldsymbol{\lambda}$, $\boldsymbol{\lambda}^\mathbf{d}$ and their derivatives at time t_k. Therefore Equations 3.42 and 3.43 can be written as

$$\begin{aligned}\mathbf{z_{k+1}} = \mathbf{z_a} + \dot{\mathbf{z}}_\mathbf{a}(t_{k+1} - t_a) + \ddot{\mathbf{y}}_\mathbf{k}^\mathbf{d} - \ddot{\mathbf{y}}_\mathbf{a}^\mathbf{d} - \dddot{\mathbf{y}}_\mathbf{a}^\mathbf{d}(t_{k+1} - t_a) \\ + \mathbf{C_1}\left[\left(\dot{\mathbf{y}}_\mathbf{k}^\mathbf{d} - \dot{\mathbf{y}}_\mathbf{k}\right) - \left(\dot{\mathbf{y}}_\mathbf{a}^\mathbf{d} - \dot{\mathbf{y}}_\mathbf{a}\right) - \left(\ddot{\mathbf{y}}_\mathbf{a}^\mathbf{d} - \ddot{\mathbf{y}}_\mathbf{a}\right)(t_{k+1} - t_a)\right] \\ + \mathbf{C_2}\left[\left(\mathbf{y}_\mathbf{k}^\mathbf{d} - \mathbf{y}_\mathbf{k}\right) - \left(\mathbf{y}_\mathbf{a}^\mathbf{d} - \mathbf{y}_\mathbf{a}\right) - \left(\dot{\mathbf{y}}_\mathbf{a}^\mathbf{d} - \dot{\mathbf{y}}_\mathbf{a}\right)(t_{k+1} - t_a)\right] \\ - \mathbf{C_3}\left(\mathbf{y}_\mathbf{a}^\mathbf{d} - \mathbf{y}_\mathbf{a}\right)(t_{k+1} - t_a) + \mathbf{C_3}(h\ddot{\mathbf{w}}_\mathbf{k+1} + \dot{\mathbf{w}}_\mathbf{k}) \\ + \mathbf{C_4}(h^2\ddot{\mathbf{w}}_\mathbf{k+1} + h\dot{\mathbf{w}}_\mathbf{k} + \mathbf{w}_\mathbf{k})\end{aligned} \tag{3.44}$$

where $\ddot{\mathbf{w}}_\mathbf{k+1} = \mathbf{y}_\mathbf{k}^\mathbf{d} - \mathbf{y}_\mathbf{k}$ and,

$$\Gamma_{k+1} = \Gamma_a + \dot{\Gamma}_a(t_{k+1} - t_a) + \lambda_k^d - \lambda_a^d - \dot{\lambda}_a^d(t_{k+1} - t_a) - \mathbf{B_1}(\lambda_a^d - \lambda_a)(t_{k+1} - t_a) + \mathbf{B_1}(h\ddot{p}_{k+1} + \dot{p}_k) + \mathbf{C_4}(h^2\ddot{p}_{k+1} + h\dot{p}_k + p_k) \tag{3.45}$$

where $\ddot{p}_{k+1} = \lambda_k^d - \lambda_k$.

It should be noted that since control torques cannot effect the end-effector accelerations, jerks, contact forces and its derivatives, any jump or step change in $\mathbf{z_{k+1}}$, Γ_{k+1}, $\dot{\boldsymbol{z}}_{\mathbf{k+1}}$ and $\dot{\Gamma}_{k+1}$ will result with infinitely large input torque requirements. To be away from this condition, $\mathbf{z_{k+1}}$, Γ_{k+1}, $\dot{\boldsymbol{z}}_{\mathbf{k+1}}$ and $\dot{\Gamma}_{k+1}$ are matched at the discontinuities of the desired trajectories. This is obtained by freely selecting the integration constants such that $\mathbf{z_a} = \mathbf{z}(t_a^+) = \mathbf{z}(t_a^-)$, $\dot{\mathbf{z}}_\mathbf{a} = \dot{\mathbf{z}}(t_a^+) = \dot{\mathbf{z}}(t_a^-)$, $\Gamma_a = \Gamma(t_a^+) = \Gamma(t_a^-)$ and $\dot{\Gamma}_a = \dot{\Gamma}(t_a^+) = \dot{\Gamma}(t_a^-)$. If the system is at rest initially, therefore, $\mathbf{z_a} = 0$, $\dot{\mathbf{z}}_\mathbf{a} = 0$, $\Gamma_a = 0$, $\dot{\Gamma}_a = 0$.

Equations 3.40 and 3.41 represent *n* number of nonlinear algebraic equations which *n* dimensional vector $\dot{\mathbf{q}}_{\mathbf{k+1}}$ can be solved. Measured $\mathbf{q_k}$ and $\dot{\mathbf{q}}_\mathbf{k}$ are used to find $\mathbf{y_k}$ and $\dot{\mathbf{y}}_\mathbf{k}$ to obtain $\mathbf{z_{k+1}}$ which is expressed in Equation 3.44 and used in Equation 3.41.

After obtaining $\dot{\mathbf{q}}_{\mathbf{k+1}}$, $\dot{\boldsymbol{\phi}}_{\mathbf{k+1}}$ is calculated by using Equation 3.38 as follows.

$$\dot{\boldsymbol{\phi}}_{\mathbf{k+1}} = (\mathbf{K}h + \mathbf{D})^{-1}\left[\mathbf{M}^* \frac{1}{h}(\dot{\mathbf{q}}_{\mathbf{k+1}} - \dot{\mathbf{q}}_\mathbf{k}) + \mathbf{Q}^* + \mathbf{K}(\mathbf{q_k} - \boldsymbol{\phi}_\mathbf{k}) + \mathbf{E}^{*\mathbf{T}}\boldsymbol{\Gamma}_{\mathbf{k+1}}\right] + \dot{\mathbf{q}}_{\mathbf{k+1}} \tag{3.46}$$

$\boldsymbol{\Gamma}_{\mathbf{k+1}}$ can be obtained from Equation 3.45. The required contact force λ_k value for calculation of command contact forces $\boldsymbol{\Gamma}_{\mathbf{k+1}}$ does not need to be measured since it can be calculated from measured quantities. Solving Equation 3.22 for $\ddot{\mathbf{q}}$ and inserting into Equation 3.10 in time t_k yields the following expression.

$$\lambda_k = \left(\mathbf{E}^*\mathbf{M}^{*-\mathbf{1}}\mathbf{E}^{*\mathbf{T}}\right)^{-1}\left\{-\mathbf{E}^*\mathbf{M}^{*-\mathbf{1}}\left[\mathbf{Q}^* + \mathbf{D}^\mathbf{a}\left(\dot{\mathbf{q}}_\mathbf{k} - \dot{\boldsymbol{\phi}}_\mathbf{k}\right) + \mathbf{K}(\mathbf{q_k} - \boldsymbol{\phi}_\mathbf{k})\right] + \dot{\mathbf{E}}^*\dot{\mathbf{q}}_\mathbf{k} + \dot{\mathbf{G}}\right\} \tag{3.47}$$

where $\mathbf{M}^*, \mathbf{Q}^*, \mathbf{E}^*, \dot{\mathbf{E}}^*$ and $\dot{\mathbf{G}}$ are calculated at time t_k.

Finally, Equation 3.39 is utilized to compute the control torques $\mathbf{T_{k+1}}$.

3.3 Error Dynamics

Command jerk rates and command contact force second derivatives are specified in the previous section and system is linearized and decoupled with the computed torques.

Let e_p and e_f represent the deviations of the measured position and contact forces from the desired ones as follows.

$$e_p = y^d - y \tag{3.48}$$

$$e_f = \lambda^d - \lambda \tag{3.49}$$

Assume that there is no modeling error and disturbances in the system. After application of control torques, this condition will lead to the actual accelerations and contact forces to be equal to z and Γ respectively, i.e. $\ddot{y} = z$ and $\lambda = \Gamma$. Therefore following error dynamics is obtained by using Equations 3.31 and 3.32.

$$e_p^{(4)} + C_1 \dddot{e}_p + C_2 \ddot{e}_p + C_3 \dot{e}_p + C_4 e_p = 0 \tag{3.50}$$

$$\ddot{e}_f + B_1 \dot{e}_f + B_2 e_f = 0 \tag{3.51}$$

Asymptotic stability is realized by an appropriate selection of feedback gains. To do this, performance indices such as Integral Square Error (ISE), Integral of the Absolute Magnitude of Error (IAE), Integral Time Absolute Error (ITAE) and Integral Time Square Error (ITSE) can be utilized. In this study ITAE performance index which is shown below will be utilized.

$$ITAE = \int_0^T t|e(t)|\,dt \tag{3.52}$$

By using ITAE performance index, due to the multiplication by time *t*, effect of large initial error is reduced while small errors in long-term are penalized.

The form of the characteristic equation based on the ITAE criterion for a closed-loop system is $s^n + C_1 s^{n-1} + C_2 s^{n-2} + \cdots + C_n$. The coefficients for a second order and fourth order systems according to ITAE are given below[15].

Table 3.1 Feedback Gains

Feedback Gains	**Second Order system**	**Fourth Order System**
B_1, C_1	$1.4\omega_0$	$2.1\ \omega_0$
B_2, C_2	ω_0^2	$3.4\ \omega_0^2$
C_3	-	$2.7\ \omega_0^3$
C_4	-	ω_0^4

where ω_0 is a constant value.

CHAPTER 4

CASE STUDY AND SIMULATIONS

4.1 Case Study

To demonstrate and evaluate the performance of the control law explained in the previous chapters, a planar parallel manipulator shown in Fig.4.1 is considered. Classification of parallel manipulators is usually according to the number of legs from the fixed base to the moving platform, and the number and type of the joints that these legs have. The parallel manipulator to be studied is called as a 2-RRR parallel manipulator which means that it has two legs and each of them has three revolute joints from the fixed base to the moving platform.

The planar parallel manipulator's end-effector is in contact with a defined surface which is a fixed plane parallel to the *x*-*z* plane for this case study. The contact force which is perpendicular to that surface is imposed on the system.

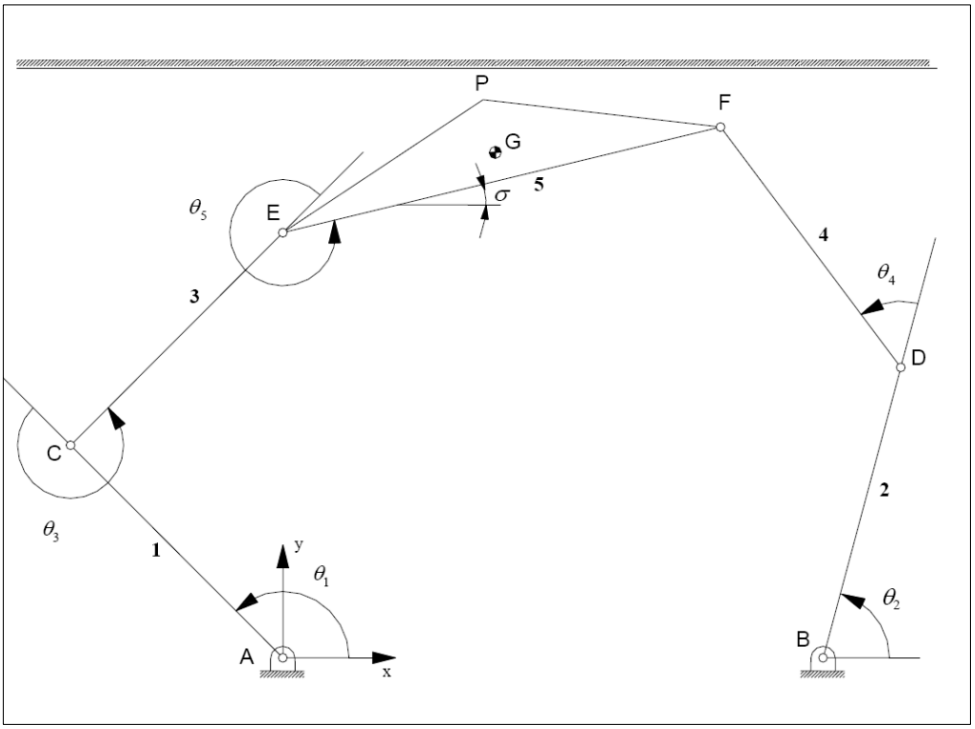

Figure 4.1 2-RRR Parallel Manipulator

The system has six links including the fixed link and six revolute joints. It is actuated by three actuators placed at A, B and C whose joint variables are θ_1, θ_2 and θ_3. The manipulator has three degrees of freedom. Additional degrees of freedom take place due to flexible joints which increases the degrees of freedom of the system to six. Rotation of the actuators is perpendicular to the plane of motion and the weights act in $-y$ direction.

The viscous damping of the actuators and the torsional damping characteristics of the structural members in the drive train are included in the dynamic model.

Let the sets of generalized coordinates corresponding to the manipulator and actuator variables expressed respectively as follows.

$$G_1 = \{\theta_1, \theta_2, \theta_3, \theta_4, \theta_5\} \tag{4.1}$$

$$G_2 = \{\phi_1, \phi_2, \phi_3\} \tag{4.2}$$

The vector of manipulator variables for the rigid links can be written as

$$\boldsymbol{\theta} = [\theta_1 \quad \theta_2 \quad \theta_3 \quad \theta_4 \quad \theta_5]^T \tag{4.3}$$

which can be partitioned into two subvectors according to actuated and unactuated joint variables as follows.

$$\boldsymbol{\theta} = [\mathbf{q} \quad \boldsymbol{\theta}^{\mathbf{u}}]^T \tag{4.4}$$

where,

$$\mathbf{q} = [\theta_1 \quad \theta_2 \quad \theta_3]^T \tag{4.5}$$

$$\boldsymbol{\theta}^{\mathbf{u}} = [\theta_4 \quad \theta_5]^T \tag{4.6}$$

The vector of actuator variables are expressed as

$$\boldsymbol{\phi} = [\phi_1 \quad \phi_2 \quad \phi_3]^T \tag{4.7}$$

The manipulator has three degrees of freedom, i.e. $n = 3$ excluding the additional degrees of freedom that come up due to the flexible joints and five joint variables are defined, i.e. $m = 5$. This leads to two constraint equations since $m - n = 2$ after disconnecting the joint at point F to get two open kinematic chains. These open kinematic chains with the unit vectors are shown in Fig. 4.2 and Fig. 4.3. In the figures, λ and $\boldsymbol{\mu_i}$, i = 1, 2 stand for the contact force perpendicular to the constraint surface and the forces apply to the disconnected joints in horizontal and vertical directions respectively.

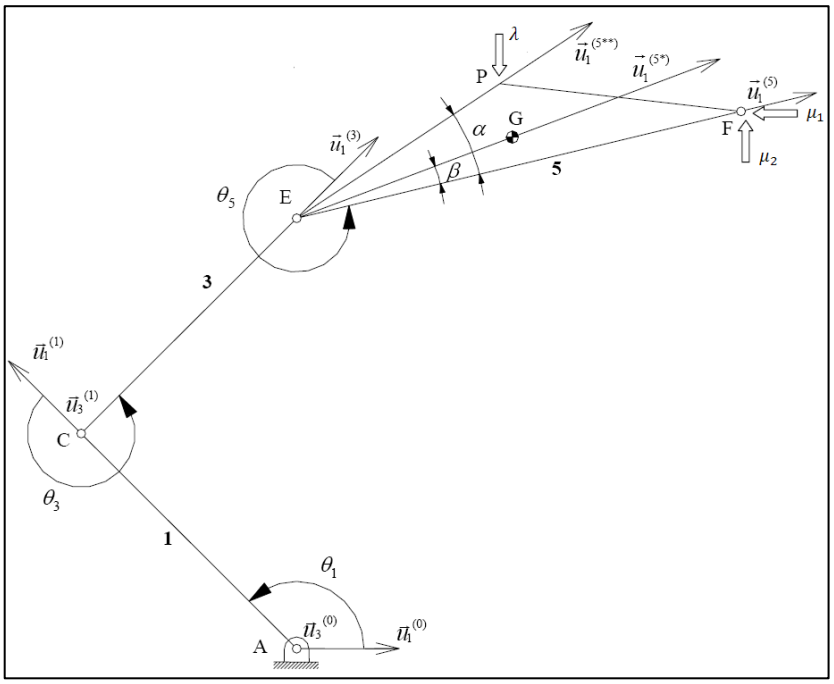

Figure 4.2 First Open Kinematic Chain

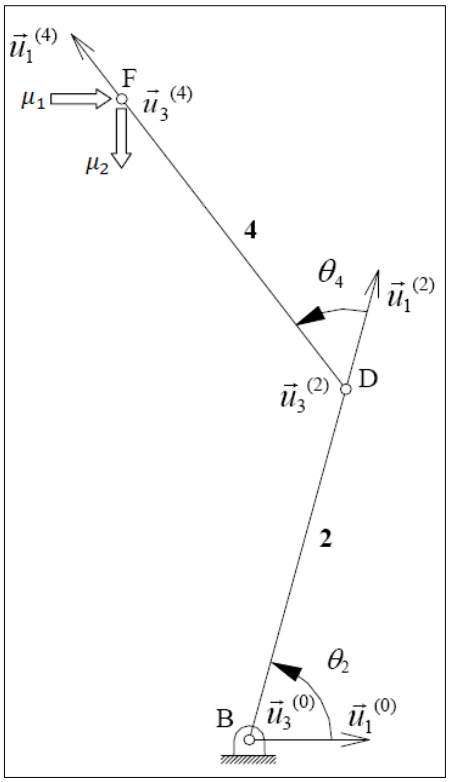

Figure 4.3 Second Open Kinematic Chain

As described in Chapter 2, equations of motion for the system are going to be derived by using the Lagrangian formulation in the following sections.

4.1.1 Kinetic Energy

Kinetic energy expressions are obtained by substituting the translational and angular velocity components for each link and actuator into Equations 2.9 and 2.20 as shown below.

Link-1

$$\bar{r}_{G_1}^{(0)} = \frac{L_1}{2}(\bar{u}_1 c\theta_1 + \bar{u}_2 s\theta_1) \tag{4.8}$$

$$\bar{V}_{G_1}^{(0)} = \dot{\bar{r}}_{G_1}^{(0)} = \frac{L_1}{2}\left(-\bar{u}_1 s\theta_1\dot{\theta}_1 + \bar{u}_2 c\theta_1\dot{\theta}_1\right) = \begin{bmatrix} -\frac{L_1}{2}s\theta_1\dot{\theta}_1 \\ \frac{L_1}{2}c\theta_1\dot{\theta}_1 \\ 0 \end{bmatrix} \tag{4.9}$$

$$\bar{\omega}_1^{(0)} = \dot{\theta}_1\bar{u}_3 = \begin{bmatrix} 0 \\ 0 \\ \dot{\theta}_1 \end{bmatrix} \tag{4.10}$$

Therefore kinetic energy of Link-1 is expressed as

$$KE_{L1} = \frac{1}{2}\left[m_1^L\frac{L_1^2}{4} + I_{1zz}\right]\dot{\theta}_1^2 \tag{4.11}$$

Link-2

$$\bar{r}_{G_2}^{(0)} = d_0\bar{u}_1 + \frac{L_2}{2}(\bar{u}_1 c\theta_2 + \bar{u}_2 s\theta_2) \tag{4.12}$$

$$\bar{V}_{G_2}^{(0)} = \dot{\bar{r}}_{G_2}^{(0)} = \frac{L_2}{2}\left(-\bar{u}_1 s\theta_2\dot{\theta}_2 + \bar{u}_2 c\theta_2\dot{\theta}_2\right) = \begin{bmatrix} -\frac{L_2}{2}s\theta_2\dot{\theta}_2 \\ \frac{L_2}{2}c\theta_2\dot{\theta}_2 \\ 0 \end{bmatrix} \tag{4.13}$$

$$\bar{\omega}_2^{(0)} = \dot{\theta}_2 \bar{u}_3 = \begin{bmatrix} 0 \\ 0 \\ \dot{\theta}_2 \end{bmatrix} \tag{4.14}$$

Therefore kinetic energy of Link-2 is expressed as

$$KE_{L2} = \frac{1}{2}\left[m_2^L \frac{L_2^2}{4} + I_{2zz}\right]\dot{\theta}_2^2 \tag{4.15}$$

Link-3

$$\bar{r}_{G_3}^{(0)} = L_1(\bar{u}_1 c\theta_1 + \bar{u}_2 s\theta_1) + \frac{L_3}{2}(\bar{u}_1 c\theta_{13} + \bar{u}_2 s\theta_{13}) \tag{4.16}$$

$$\bar{V}_{G_3}^{(0)} = \dot{\bar{r}}_{G_3}^{(0)} = L_1\left(-\bar{u}_1 s\theta_1 \dot{\theta}_1\right) + \frac{L_3}{2}\left(-\bar{u}_1 s\theta_{13}\dot{\theta}_{13} + \bar{u}_2 c\theta_{13}\dot{\theta}_{13}\right)$$

$$= \begin{bmatrix} -L_1 s\theta_1 \dot{\theta}_1 - \frac{L_3}{2} s\theta_{13}\dot{\theta}_{13} \\ L_1 c\theta_1 \dot{\theta}_1 + \frac{L_2}{2} c\theta_{13}\dot{\theta}_{13} \\ 0 \end{bmatrix} \tag{4.17}$$

$$\bar{\omega}_3^{(0)} = \dot{\theta}_1 \bar{u}_{3+} \dot{\theta}_3 \bar{u}_3 = \begin{bmatrix} 0 \\ 0 \\ \dot{\theta}_{13} \end{bmatrix} \tag{4.18}$$

Therefore kinetic energy of Link-3 is expressed as

$$KE_{L3} = \frac{1}{2} m_3^L L_1^2 \dot{\theta}_1^{\,2} + \frac{1}{2} m_3^L L_1 L_3 c(\theta_1 - \theta_{13})\dot{\theta}_1\left(\dot{\theta}_1 + \dot{\theta}_3\right) + \frac{1}{2}\left[m_3^L \frac{L_3^2}{4} + I_{3zz}\right]\left(\dot{\theta}_1 + \dot{\theta}_3\right)^2 \tag{4.19}$$

Above expression can be written in expanded form as follows.

$$KE_{L3} = \frac{1}{2}m_3^L L_1^2\dot{\theta}_1^2 + \frac{1}{2}m_3^L L_1 L_3 c(-\theta_3)\dot{\theta}_1^2 + \frac{1}{2}m_3^L L_1 L_3 c(-\theta_3)\dot{\theta}_1\dot{\theta}_3 + \frac{1}{2}\left[m_3^L\frac{L_3^2}{4} + I_{3zz}\right]\dot{\theta}_1^2 + \left[m_3^L\frac{L_3^2}{4} + I_{3zz}\right]\dot{\theta}_1\dot{\theta}_3 + \frac{1}{2}\left[m_3^L\frac{L_3^2}{4} + I_{3zz}\right]\dot{\theta}_3^2 \quad (4.20)$$

Link-4:

$$\bar{r}_{G_4}^{(0)} = d_0\bar{u}_1 + L_2(\bar{u}_1 c\theta_2 + \bar{u}_2 s\theta_2) + \tfrac{L_4}{2}(\bar{u}_1 c\theta_{24} + \bar{u}_2 s\theta_{24}) \quad (4.21)$$

$$\bar{V}_{G_4}^{(0)} = \dot{\bar{r}}_{G_4}^{(0)} = L_2\left(-\bar{u}_1 s\theta_2\dot{\theta}_2 + \bar{u}_2 c\theta_2\dot{\theta}_2\right) + \frac{L_4}{2}\left(-\bar{u}_1 s\theta_{24}\dot{\theta}_{24} + \bar{u}_2 c\theta_{24}\dot{\theta}_{24}\right) = \begin{bmatrix} -L_2 s\theta_2\dot{\theta}_2 - \frac{L_4}{2}s\theta_{24}\dot{\theta}_{24} \\ L_2 c\theta_2\dot{\theta}_2 + \frac{L_4}{2}c\theta_{24}\dot{\theta}_{24} \\ 0 \end{bmatrix} \quad (4.22)$$

$$\bar{\omega}_4^{(0)} = \dot{\theta}_2\bar{u}_{3+}\dot{\theta}_4\bar{u}_3 = \begin{bmatrix} 0 \\ 0 \\ \dot{\theta}_{24} \end{bmatrix} \quad (4.23)$$

Therefore kinetic energy of Link-4 is expressed as

$$KE_{L4} = \frac{1}{2}m_4^L L_2^2\dot{\theta}_2^{\,2} + \frac{1}{2}m_4^L L_2 L_4 c(\theta_2 - \theta_{24})\dot{\theta}_2\left(\dot{\theta}_2 + \dot{\theta}_{24}\right) + \frac{1}{2}\left[m_4^L\frac{L_4^2}{4} + I_{4zz}\right]\left(\dot{\theta}_2 + \dot{\theta}_4\right)^2 \quad (4.24)$$

Above expression can be written in expanded form as follows.

$$KE_{L4} = \frac{1}{2}m_4^L L_2^2\dot{\theta}_2^2 + \frac{1}{2}m_4^L L_2 L_4 c(-\theta_4)\dot{\theta}_2^2 + \frac{1}{2}m_4^L L_2 L_4 c(-\theta_4)\dot{\theta}_2\dot{\theta}_4 + \frac{1}{2}\left[m_4^L\frac{L_4^2}{4} + I_{4zz}\right]\dot{\theta}_2^2 + \left[m_4^L\frac{L_4^2}{4} + I_{4zz}\right]\dot{\theta}_2\dot{\theta}_4 + \frac{1}{2}\left[m_4^L\frac{L_4^2}{4} + I_{4zz}\right]\dot{\theta}_4^2 \quad (4.25)$$

Link-5:

$$\bar{r}_{G_5}^{(0)} = L_1(\bar{u}_1 c\theta_1 + \bar{u}_2 s\theta_1) + L_3(\bar{u}_1 c\theta_{13} + \bar{u}_2 s\theta_{13}) + g_5[\bar{u}_1 c(\theta_{135} + \beta) + \bar{u}_2 s(\theta_{135} + \beta)] \quad (4.26)$$

$$\bar{V}_{G_5}^{(0)} = \dot{\bar{r}}_{G_5}^{(0)}$$
$$= L_1\left(-\bar{u}_1 s\theta_1\dot{\theta}_1 + \bar{u}_2 c\theta_1\dot{\theta}_1\right) + L_3\left(-\bar{u}_1 s\theta_{13}\dot{\theta}_{13} + \bar{u}_2 c\theta_{13}\dot{\theta}_{13}\right)$$
$$+ g_5\left[\bar{u}_1 s(\theta_{135} + \beta)\dot{\theta}_{135} + \bar{u}_2 c(\theta_{135} + \beta)\dot{\theta}_{135}\right]$$
$$= \begin{bmatrix} -L_1 s\theta_1\dot{\theta}_1 - L_3 s\theta_{13}\dot{\theta}_{13} - g_5 s(\theta_{135} + \beta)\dot{\theta}_{135} \\ L_1 c\theta_1\dot{\theta}_1 + L_3 c\theta_{13}\dot{\theta}_{13} + g_5 c(\theta_{135} + \beta)\dot{\theta}_{135} \\ 0 \end{bmatrix} \quad (4.27)$$

$$\bar{\omega}_5^{(0)} = \dot{\theta}_1\bar{u}_{3+} + \dot{\theta}_3\bar{u}_3 + \dot{\theta}_5\bar{u}_{3+} = \begin{bmatrix} 0 \\ 0 \\ \dot{\theta}_{135} \end{bmatrix} \quad (4.28)$$

Therefore kinetic energy of Link-5 is expressed as

$$KE_{L5} = \frac{1}{2}m_5^L L_1^2\dot{\theta}_1^2 + \frac{1}{2}m_5^L L_3^2\left(\dot{\theta}_1 + \dot{\theta}_3\right)^2 + \frac{1}{2}[m_5^L g_5^2 + I_{5zz}]\left(\dot{\theta}_1 + \dot{\theta}_3 + \dot{\theta}_5\right)^2 + m_5^L L_1 L_3 c(\theta_1 - \theta_{13})\dot{\theta}_1\left(\dot{\theta}_1 + \dot{\theta}_3\right) + m_5^L L_1 g_5 c(\theta_1 - \theta_{135} - \beta)\dot{\theta}_1\left(\dot{\theta}_1 + \dot{\theta}_3 + \dot{\theta}_5\right) + m_5^L L_3 g_5 c(\theta_{13} - \theta_{135} - \beta)\left(\dot{\theta}_1 + \dot{\theta}_3\right) \quad (4.29)$$

Above expression can be written in expanded form as follows.

$$KE_{L5} = \tfrac{1}{2}m_5^L L_1^2\dot{\theta}_1^2 + \tfrac{1}{2}m_5^L L_3^2\dot{\theta}_1^2 + m_5^L L_3^2\dot{\theta}_1\dot{\theta}_3 + \tfrac{1}{2}m_5^L L_3^2\dot{\theta}_3^2 + \tfrac{1}{2}[m_5^L g_5^2 + I_{5zz}]\dot{\theta}_1^2 + \tfrac{1}{2}[m_5^L g_5^2 + I_{5zz}]\dot{\theta}_3^2 + \tfrac{1}{2}[m_5^L g_5^2 + I_{5zz}]\dot{\theta}_5^2 + [m_5^L g_5^2 + I_{5zz}]\dot{\theta}_1\dot{\theta}_3 + [m_5^L g_5^2 + I_{5zz}]\dot{\theta}_1\dot{\theta}_5 + [m_5^L g_5^2 + I_{5zz}]\dot{\theta}_3\dot{\theta}_5 + m_5^L L_1 L_3 c(-\theta_3)\dot{\theta}_1^2 + m_5^L L_1 L_3 c(-\theta_3)\dot{\theta}_1\dot{\theta}_3 + m_5^L L_1 g_5 c[-(\theta_3 + \theta_5 + \beta)]\dot{\theta}_1^2 + m_5^L L_1 g_5 c[-(\theta_3 + \theta_5 + \beta)]\dot{\theta}_1\dot{\theta}_3 + m_5^L L_1 g_5 c[-(\theta_3 + \theta_5 + \beta)]\dot{\theta}_1\dot{\theta}_5 + m_5^L L_3 g_5 c[-(\theta_5 + \beta)]\dot{\theta}_1^2 + m_5^L L_3 g_5 c[-(\theta_5 + \beta)]\dot{\theta}_1\dot{\theta}_3 + m_5^L L_3 g_5 c[-(\theta_5 + \beta)]\dot{\theta}_1\dot{\theta}_5 + m_5^L L_3 g_5 c[-(\theta_5 + \beta)]\dot{\theta}_1\dot{\theta}_3 + m_5^L L_3 g_5 c[-(\theta_5 + \beta)]\dot{\theta}_3^2 + m_5^L L_3 g_5 c[-(\theta_5 + \beta)]\dot{\theta}_3\dot{\theta}_5 \quad (4.30)$$

Actuator-1:

$$\bar{V}_1^A = 0 \quad (4.31)$$

$$\bar{\omega}_1^A = \begin{bmatrix} 0 \\ 0 \\ r_1\dot{\phi}_1 \end{bmatrix} \quad (4.32)$$

Therefore kinetic energy of Actuator-1 is expressed as

$$KE_{A1} = \frac{1}{2}[r_1^2 I_{1zz}^r]\dot{\phi}_2^2 \quad (4.33)$$

Actuator-2:

$$\bar{V}_2^A = 0 \tag{4.34}$$

$$\bar{\omega}_1^A = \begin{bmatrix} 0 \\ 0 \\ r_2\dot{\phi}_2 \end{bmatrix} \tag{4.35}$$

Therefore kinetic energy of Actuator-2 is expressed as

$$KE_{A2} = \frac{1}{2}[r_2^2 I_{2zz}^r]\dot{\phi}_2^2 \tag{4.36}$$

Actuator-3:

$$\bar{V}_3^A = \begin{bmatrix} -L_1 s\theta_1\dot{\theta}_1 \\ L_1 c\theta_1\dot{\theta}_1 \\ 0 \end{bmatrix} \tag{4.37}$$

$$\bar{\omega}_1^A = \begin{bmatrix} 0 \\ 0 \\ r_3\dot{\phi}_3 \end{bmatrix} \tag{4.38}$$

Therefore kinetic energy of Actuator-3 is expressed as

$$KE_{A3} = \frac{1}{2}[m_3^A L_1^2 + I_{3zz}^r]\dot{\theta}_1^2 + \frac{1}{2}[r_3^2 I_{3zz}^r]\dot{\phi}_3^2 \tag{4.39}$$

Total kinetic energy of the system is the sum of all kinetic energy contributions of links and actuators.

The Lagrange components related to the kinetic energy are given below.

$$\frac{d}{dt}\left(\frac{\partial K}{\partial \dot{\theta}_1}\right) = \ddot{\theta}_1 \left\{\left[m_1^L \frac{{L_1}^2}{4} + I_{1zz}\right] + m_3^L {L_1}^2 + m_3^L L_1 L_3 c(-\theta_3)\right.$$

$$+\left[m_3^L \frac{{L_3}^2}{4} + I_{3zz}\right] + m_5^L {L_1}^2 + m_5^L {L_3}^2 + [m_5^L g_5^2 + I_{5zz}]$$

$$+2m_5^L L_1 L_3 c(-\theta_3) + 2m_5^L L_1 g_5 c[-(\theta_3 + \theta_5 + \beta)]$$

$$\left.+2m_5^L L_3 g_5 c[-(\theta_5 + \beta)] + m_3^A {L_1}^2 + {I^r}_{3zz}\right\}$$

$$+\ddot{\theta}_3 \left\{m_3^L \frac{L_1}{2} L_3 c(-\theta_3) + \left[m_3^L \frac{L_3^2}{4} + I_{3zz}\right] + m_5^L {L_3}^2\right.$$

$$+[m_5^L g_5^2 + I_{5zz}] + m_5^L L_1 L_3 c(-\theta_3)$$

$$\left.+m_5^L L_1 g_5 c[-(\theta_3 + \theta_5 + \beta)]+2m_5^L L_3 g_5 c[-(\theta_5 + \beta)]\right\}$$

$$+\ddot{\theta}_5\{[m_5^L g_5^2 + I_{5zz}] +m_5^L L_1 g_5 c[-(\theta_3 + \theta_5 + \beta)]$$

$$+m_5^L L_3 g_5 c[-(\theta_5 + \beta)]$$

(4.40)

$$\frac{d}{dt}\left(\frac{\partial K}{\partial \dot{\theta}_2}\right) = \ddot{\theta}_2 \left\{\left[{m_2}^L \frac{{L_2}^2}{4} + I_{2zz}\right] + {m_4}^L {L_2}^2 + {m_4}^L L_2 L_4 c(-\theta_4)\right.$$

$$\left.+\left[{m_4}^L \frac{{L_4}^2}{4} + I_{4zz}\right]\right\}$$

$$+\ddot{\theta}_4 \left\{\frac{1}{2}{m_4}^L L_2 L_4 c(-\theta_4) + \left[{m_4}^L \frac{{L_4}^2}{4} + I_{4zz}\right]\right\}$$

(4.41)

$$\frac{d}{dt}\left(\frac{\partial K}{\partial \dot{\theta}_3}\right) = \ddot{\theta}_3 \left\{\left[{m_3}^L \frac{{L_3}^2}{4} + I_{3zz}\right] + {m_5}^L {L_3}^2 + [{m_5}^L {g_5}^2 + I_{5zz}]\right.$$
$$\left. + 2{m_5}^L L_3 g_5 c[-(\theta_5 + \beta)]\right\}$$
$$+ \ddot{\theta}_1 \left\{{m_3}^L \frac{L_1}{2} L_3 c(-\theta_3) + \left[{m_3}^L \frac{{L_3}^2}{4} + I_{3zz}\right] + {m_5}^L {L_3}^2\right.$$
$$+ [{m_5}^L {g_5}^2 + I_{5zz}] + {m_5}^L L_1 L_3 c(-\theta_3)$$
$$\left. + {m_5}^L L_1 g_5 c[-(\theta_3 + \theta_5 + \beta)] + 2{m_5}^L L_3 g_5 c[-(\theta_5 + \beta)]\right\}$$
$$+ \ddot{\theta}_5\{[{m_5}^L {g_5}^2 + I_{5zz}] + {m_5}^L L_3 g_5 c[-(\theta_5 + \beta)]\}$$

(4.42)

$$\frac{d}{dt}\left(\frac{\partial K}{\partial \dot{\theta}_4}\right) = \ddot{\theta}_4 \left\{\left[{m_4}^L \frac{{L_4}^2}{4} + I_{4zz}\right]\right\}$$
$$+ \ddot{\theta}_2 \left\{\frac{1}{2}{m_4}^L L_2 L_4 c(-\theta_4) + \left[{m_4}^L \frac{{L_4}^2}{4} + I_{4zz}\right]\right\}$$

(4.43)

$$\frac{d}{dt}\left(\frac{\partial K}{\partial \dot{\theta}_5}\right) = \ddot{\theta}_5\{[{m_5}^L {g_5}^2 + I_{5zz}]\}$$
$$+ \ddot{\theta}_1\{[{m_5}^L {g_5}^2 + I_{5zz}] + {m_5}^L L_1 g_5 c[-(\theta_3 + \theta_5 + \beta)]$$
$$+ {m_5}^L L_3 g_5 c[-(\theta_5 + \beta)]\}$$
$$+ \ddot{\theta}_3\{[{m_5}^L {g_5}^2 + I_{5zz}] + {m_5}^L L_3 g_5 c[-(\theta_5 + \beta)]\}$$

(4.44)

$$\frac{d}{dt}\left(\frac{\partial K}{\partial \dot{\phi}_1}\right) = \ddot{\phi}_1\{{r_1}^2 {I^r}_{1zz}\} \tag{4.45}$$

$$\frac{d}{dt}\left(\frac{\partial K}{\partial \dot{\phi}_2}\right) = \ddot{\phi}_2\{{r_2}^2 {I^r}_{2zz}\} \tag{4.46}$$

$$\frac{d}{dt}\left(\frac{\partial K}{\partial \dot{\phi}_3}\right) = \ddot{\phi}_3\{{r_3}^2 {I^r}_{3zz}\} \tag{4.47}$$

$$\frac{\partial K}{\partial \theta_1} = 0 \tag{4.48}$$

$$\frac{\partial K}{\partial \theta_2} = 0 \tag{4.49}$$

$$\begin{aligned}\frac{\partial K}{\partial \theta_3} = \frac{1}{2}{\dot{\theta}_1}^2 \{ & {m_3}^L L_1 L_3 s(-\theta_3) + 2{m_5}^L L_1 L_3 s(-\theta_3) \\ & + 2{m_5}^L L_1 g_5 s[-(\theta_3 + \theta_5 + \beta)]\} \\ & + \dot{\theta}_1 \dot{\theta}_3 \left\{\frac{1}{2}{m_3}^L L_1 L_3 s(-\theta_3) + {m_5}^L L_1 L_3 s(-\theta_3)\right. \\ & \left. + {m_5}^L L_1 g_5 s[-(\theta_3 + \theta_5 + \beta)]\right\} \\ & + \dot{\theta}_1 \dot{\theta}_5 \{{m_5}^L L_1 g_5 s[-(\theta_3 + \theta_5 + \beta)]\}\end{aligned} \tag{4.50}$$

$$\frac{\partial K}{\partial \theta_4} = \frac{1}{2}{\dot{\theta}_2}^2 {m_4}^L L_2 L_4 s(-\theta_4) + \dot{\theta}_2 \dot{\theta}_4 \frac{1}{2}{m_4}^L L_2 L_4 s(-\theta_4) \tag{4.51}$$

$$\frac{\partial K}{\partial \theta_5} = \dot{\theta_2}^2\{m_5{}^L L_1 g_5 s[-(\theta_3+\theta_5+\beta)] + m_5{}^L L_3 g_5 s[-(\theta_5+\beta)]\}$$
$$+ \dot{\theta_3}^2\{m_5{}^L L_3 g_5 s[-(\theta_5+\beta)]\}$$
$$+ \dot{\theta}_1\dot{\theta}_3\{m_5{}^L L_1 g_5 s[-(\theta_3+\theta_5+\beta)]$$
$$+ 2m_5{}^L L_3 g_5 s[-(\theta_5+\beta)]\}$$
$$+ \dot{\theta}_1\dot{\theta}_5\{m_5{}^L L_1 g_5 s[-(\theta_3+\theta_5+\beta)] + m_5{}^L L_3 g_5 s[-(\theta_5+\beta)]\}$$
$$+ \dot{\theta}_3\dot{\theta}_5\{m_5{}^L L_3 g_5 s[-(\theta_5+\beta)]\} \quad (4.52)$$

4.1.2 Potential Energy

Potential energy expressions for links and actuators are given below.

$$PE_{L1} = m_1{}^L g\left(\frac{L_1}{2} s\theta_1\right) \quad (4.53)$$

$$PE_{L2} = m_2{}^L g\left(\frac{L_2}{2} s\theta_2\right) \quad (4.54)$$

$$PE_{L3} = m_3{}^L g\left(L_1 s\theta_1 + \frac{L_3}{2} s\theta_{13}\right) \quad (4.55)$$

$$PE_{L4} = m_4{}^L g\left(L_2 s\theta_2 + \frac{L_4}{2} s\theta_{24}\right) \quad (4.56)$$

$$PE_{L5} = m_5{}^L g[L_1 s\theta_1 + L_3 s\theta_{13} + g_5 s(\theta_{135}+\beta)] \quad (4.57)$$

$$PE_{A1} = \frac{1}{2} K_1(\phi_1 - \theta_1)^2 \quad (4.58)$$

$$PE_{A2} = \frac{1}{2} K_2(\phi_2 - \theta_2)^2 \quad (4.59)$$

$$PE_{A3} = \frac{1}{2} K_3(\phi_3 - \theta_3)^2 + m_3{}^A g(L_1 s\theta_1) \quad (4.60)$$

Total potential energy of the system is the sum of above expressions.

$$U = {m_1}^L g\left(\frac{L_1}{2}s\theta_1\right) + {m_3}^L g\left(L_1 s\theta_1 + \frac{L_3}{2}s\theta_{13}\right) + {m_5}^L g[L_1 s\theta_1 + L_3 s\theta_{13} + g_5 s(\theta_{135} + \beta)] + {m_2}^L g\left(\frac{L_2}{2}s\theta_2\right) + {m_4}^L g\left(L_2 s\theta_2 + \frac{L_4}{2}s\theta_{24}\right) + \frac{1}{2}K_1(\phi_1 - \theta_1)^2 + \frac{1}{2}K_2(\phi_2 - \theta_2)^2 + \frac{1}{2}K_3(\phi_3 - \theta_3)^2 + {m_3}^A g(L_1 s\theta_1) \quad (4.61)$$

The Lagrange components associated with total potential energy of the system are as follows.

$$\frac{\partial U}{\partial \theta_1} = {m_1}^L g\left(\frac{L_1}{2}c\theta_1\right) + {m_3}^L g\left(L_1 c\theta_1 + \frac{L_3}{2}c\theta_{13}\right) + {m_5}^L g[L_1 c\theta_1 + L_3 c\theta_{13} + g_5 c(\theta_{135} + \beta)] - K_1(\phi_1 - \theta_1) + {m_3}^A g(L_1 c\theta_1) \quad (4.62)$$

$$\frac{\partial U}{\partial \theta_2} = {m_2}^L g\left(\frac{L_2}{2}c\theta_2\right) + {m_4}^L g\left(L_2 c\theta_2 + \frac{L_4}{2}c\theta_{24}\right) - K_2(\phi_2 - \theta_2) \quad (4.63)$$

$$\frac{\partial U}{\partial \theta_3} = {m_3}^L g\left(\frac{L_3}{2}c\theta_{13}\right) + {m_5}^L g[L_3 c\theta_{13} + g_5 c(\theta_{135} + \beta)] - K_3(\phi_3 - \theta_3) \quad (4.64)$$

$$\frac{\partial U}{\partial \theta_4} = {m_2}^L g\left(\frac{L_2}{2}c\theta_2\right) + {m_4}^L g\left(L_2 c\theta_2 + \frac{L_4}{2}c\theta_{24}\right) \quad (4.65)$$

$$\frac{\partial U}{\partial \theta_5} = {m_5}^L g[g_5 c(\theta_{135} + \beta)] \quad (4.66)$$

$$\frac{\partial U}{\partial \phi_1} = K_1(\phi_1 - \theta_1) \quad (4.67)$$

$$\frac{\partial U}{\partial \phi_2} = K_2(\phi_2 - \theta_2) \quad (4.68)$$

$$\frac{\partial U}{\partial \phi_3} = K_3(\phi_3 - \theta_3) \tag{4.69}$$

4.1.3 Dissipation Function Expressions

Dissipation functions for actuated joints, unactuated joints and rotors are expressed as

$$D^a = \frac{1}{2}D_1\left(\dot{\theta}_1 - \dot{\phi}_1\right)^2 + \frac{1}{2}D_2\left(\dot{\theta}_2 - \dot{\phi}_2\right)^2 + \frac{1}{2}D_3\left(\dot{\theta}_3 - \dot{\phi}_3\right)^2 \tag{4.70}$$

$$D^u = \frac{1}{2}D_4{\dot{\theta}_4}^2 + \frac{1}{2}D_5{\dot{\theta}_5}^2 \tag{4.71}$$

$$D^r = \frac{1}{2}{D^r}_1{r_1}^2{\dot{\phi}_1}^2 + \frac{1}{2}{D^r}_2{r_2}^2{\dot{\phi}_2}^2 + \frac{1}{2}{D^r}_3{r_3}^2{\dot{\phi}_3}^2 \tag{4.72}$$

Additionally, when the disconnected joint is reconnected, dissipation function related to the viscous friction at the disconnected joint appears to be

$$D^d = \frac{1}{2}D_6\left(\dot{\theta}_4 - \dot{\theta}_5\right)^2 \tag{4.73}$$

The dissipation function of the system is the sum of above expressions. This is formulated as below.

$$D = \tfrac{1}{2}D_1\left(\dot{\theta}_1 - \dot{\phi}_1\right)^2 + \tfrac{1}{2}D_2\left(\dot{\theta}_2 - \dot{\phi}_2\right)^2 + \tfrac{1}{2}D_3\left(\dot{\theta}_3 - \dot{\phi}_3\right)^2 + \tfrac{1}{2}D_4{\dot{\theta}_4}^2 + \tfrac{1}{2}D_5{\dot{\theta}_5}^2 + \tfrac{1}{2}D_6\left(\dot{\theta}_4 - \dot{\theta}_5\right)^2 + \tfrac{1}{2}{D^r}_1{r_1}^2{\dot{\phi}_1}^2 + \tfrac{1}{2}{D^r}_2{r_2}^2{\dot{\phi}_2}^2 + \tfrac{1}{2}{D^r}_3{r_3}^2{\dot{\phi}_3}^2 \tag{4.74}$$

The Lagrange components associated with the dissipation function of the system are as follows.

$$\frac{\partial D}{\partial \dot{\theta}_1} = D_1\left(\dot{\theta}_1 - \dot{\phi}_1\right) \tag{4.75}$$

$$\frac{\partial D}{\partial \dot{\theta}_2} = D_2\left(\dot{\theta}_2 - \dot{\phi}_2\right) \tag{4.76}$$

$$\frac{\partial D}{\partial \dot{\theta}_3} = D_3\left(\dot{\theta}_3 - \dot{\phi}_3\right) \tag{4.77}$$

$$\frac{\partial D}{\partial \dot{\theta}_4} = D_4\dot{\theta}_4 + D_6\left(\dot{\theta}_4 - \dot{\theta}_5\right) = (D_4 + D_6)\dot{\theta}_4 - D_6\dot{\theta}_5 \tag{4.78}$$

$$\frac{\partial D}{\partial \dot{\theta}_5} = D_5\dot{\theta}_5 - D_6\left(\dot{\theta}_4 - \dot{\theta}_5\right) = (D_5 + D_6)\dot{\theta}_5 - D_6\dot{\theta}_4 \tag{4.79}$$

$$\frac{\partial D}{\partial \dot{\phi}_1} = -D_1\left(\dot{\theta}_1 - \dot{\phi}_1\right) + D^r{}_1 r_1{}^2\dot{\phi}_1 \tag{4.80}$$

$$\frac{\partial D}{\partial \dot{\phi}_2} = -D_2\left(\dot{\theta}_2 - \dot{\phi}_2\right) + D^r{}_2 r_2{}^2\dot{\phi}_2 \tag{4.81}$$

$$\frac{\partial D}{\partial \dot{\phi}_3} = -D_3\left(\dot{\theta}_3 - \dot{\phi}_3\right) + D^r{}_3 r_3{}^2\dot{\phi}_3 \tag{4.82}$$

4.1.4 Constraint Equations

By disconnecting the joint at point F, two open kinematic chains are obtained which lead to two constraint equations.

These constraint equations at the disconnected joint can be formulated in velocity level as in Equation 2.33.

$$L_1 c\theta_1 + L_3 c\theta_{13} + L_5 c\theta_{135} - L_2 c\theta_2 - L_4 c\theta_{24} - d_0 = 0 \tag{4.83}$$

$$L_1 s\theta_1 + L_3 s\theta_{13} + L_5 s\theta_{135} - L_2 s\theta_2 - L_4 s\theta_{24} = 0 \tag{4.84}$$

Above equations can be written in velocity level as follows.

$$-L_1 s\theta_1 \dot{\theta}_1 - L_3 s\theta_{13}\left(\dot{\theta}_1 + \dot{\theta}_3\right) - L_5 s\theta_{135}\left(\dot{\theta}_1 + \dot{\theta}_3 + \dot{\theta}_5\right) + L_2 s\theta_2 \dot{\theta}_2 + L_4 s\theta_{24}\left(\dot{\theta}_2 + \dot{\theta}_4\right) = 0 \quad (4.85)$$

$$L_1 c\theta_1 \dot{\theta}_1 + L_3 c\theta_{13}\left(\dot{\theta}_1 + \dot{\theta}_3\right) + L_5 c\theta_{135}\left(\dot{\theta}_1 + \dot{\theta}_3 + \dot{\theta}_5\right) - L_2 c\theta_2 \dot{\theta}_2 - L_4 c\theta_{24}\left(\dot{\theta}_2 + \dot{\theta}_4\right) = 0 \quad (4.86)$$

Velocity level constraint equations can be written in a matrix form as shown in Equation 2.35.

$$\begin{bmatrix} B_{11} & B_{12} & B_{13} & B_{14} & B_{15} \\ B_{21} & B_{22} & B_{23} & B_{24} & B_{25} \end{bmatrix} \begin{bmatrix} \theta_1 \\ \theta_2 \\ \theta_3 \\ \theta_4 \\ \theta_5 \end{bmatrix} = \mathbf{0} \quad (4.87)$$

where

$$B_{11} = -L_1 s\theta_1 - L_3 s\theta_{13} - L_5 s\theta_{135} \quad (4.88)$$

$$B_{12} = L_2 s\theta_2 + L_4 s\theta_{24} \quad (4.89)$$

$$B_{13} = -L_3 s\theta_{13} - L_5 s\theta_{135} \quad (4.90)$$

$$B_{14} = L_4 s\theta_{24} \quad (4.91)$$

$$B_{15} = -L_5 s\theta_{135} \quad (4.92)$$

$$B_{21} = L_1 c\theta_1 + L_3 c\theta_{13} + L_5 c\theta_{135} \quad (4.93)$$

$$B_{22} = -L_2 c\theta_2 - L_4 c\theta_{24} \quad (4.94)$$

$$B_{23} = L_3 c\theta_{13} + L_5 c\theta_{135} \quad (4.95)$$

$$B_{24} = -L_4 c\theta_{24} \quad (4.96)$$

$$B_{25} = L_5 c\theta_{135} \quad (4.97)$$

B can be subdivided into two as explained in Section 2.4 which yields the following expressions.

$$\mathbf{B^a} = \begin{bmatrix} B_{11} & B_{12} & B_{13} \\ B_{21} & B_{22} & B_{23} \end{bmatrix} \quad (4.98)$$

$$\mathbf{B^u} = \begin{bmatrix} B_{14} & B_{15} \\ B_{24} & B_{25} \end{bmatrix} \tag{4.99}$$

End-effector position can be written as below by using Equation 2.49.

$$\mathbf{x} = \begin{bmatrix} x_1 \\ x_2 \\ x_3 \end{bmatrix} = \begin{bmatrix} L_1 c\theta_1 + L_3 c\theta_{13} + d_5 s(\theta_{135} + \alpha) \\ L_1 s\theta_1 + L_3 s\theta_{13} + d_5 s(\theta_{135} + \alpha) \\ \theta_{135} \end{bmatrix} \tag{4.100}$$

where x_1, x_2 and x_3 represent the position of the end-effector in *x*-direction, the position of the end-effector in *y*-direction and the orientation of the end-effector platform.

In order to specify the generalized forces due to the contact with the defined surface, Equation 2.54 will be utilized. The contact surface is a fixed plane parallel to the *x*-*z* plane as mentioned before, therefore $r = 1$. The constraint equation describing the contact of the end-effector with the environment is given in Equation 2.50 and can be written as

$$g(x, t) = x_2 - x_{2_0} = 0 \tag{4.101}$$

where x_{2_0} is the desired constant value which describing the location of the fixed plane parallel to the *x*-*z* plane. Above equation can be written in terms of θ as

$$L_1 s\theta_1 + L_3 s\theta_{13} + d_5 s(\theta_{135} + \alpha) - x_{2_0} = 0 \tag{4.102}$$

Therefore **E** can be derived by using Equations above and 2.52.

$$\mathbf{E} = \begin{bmatrix} L_1 c\theta_1 + L_3 c\theta_{13} + d_5 s(\theta_{135} + \alpha) \\ 0 \\ L_3 c\theta_{13} + d_5 c(\theta_{135} + \alpha) \\ 0 \\ d_5 s(\theta_{135} + \alpha) \end{bmatrix}^{\mathrm{T}} \tag{4.103}$$

Independent coordinates of the end-effector along the contact surfaces are defined by using Equation 3.1.

$$\mathbf{y} = \begin{bmatrix} x_1 \\ x_3 \end{bmatrix} = \begin{bmatrix} y_1 \\ y_2 \end{bmatrix} = \begin{bmatrix} L_1 c\theta_1 + L_3 c\theta_{13} + d_5 s(\theta_{135} + \alpha) \\ \theta_{135} \end{bmatrix} \tag{4.104}$$

P can be obtained by using Equation 3.3 as follows.

$$\mathbf{P} = \begin{bmatrix} -L_1 s\theta_1 - L_3 s\theta_{13} - d_5 s(\theta_{135} + \alpha) & 1 \\ 0 & 0 \\ L_3 s\theta_{13} - d_5 s(\theta_{135} + \alpha) & 1 \\ 0 & 0 \\ -d_5 s(\theta_{135} + \alpha) & 1 \end{bmatrix}^{T} \tag{4.105}$$

4.1.5 System Equation of Motion

The system equations of motion corresponding to the first set of generalized coordinates in matrix form can be written as follows.

$$\begin{bmatrix} M_{11} & 0 & M_{13} & 0 & M_{15} \\ 0 & M_{22} & 0 & M_{24} & 0 \\ M_{13} & 0 & M_{33} & 0 & M_{35} \\ 0 & M_{24} & 0 & M_{44} & 0 \\ M_{15} & 0 & M_{35} & 0 & M_{55} \end{bmatrix} \begin{bmatrix} \ddot{\theta}_1 \\ \ddot{\theta}_2 \\ \ddot{\theta}_3 \\ \ddot{\theta}_4 \\ \ddot{\theta}_5 \end{bmatrix} + \begin{bmatrix} Q_1 \\ Q_2 \\ Q_3 \\ Q_4 \\ Q_5 \end{bmatrix} + \begin{bmatrix} Da_1 \\ Da_2 \\ Da_3 \\ Da_4 \\ Da_5 \end{bmatrix} + \begin{bmatrix} St_1 \\ St_2 \\ St_3 \\ St_4 \\ St_5 \end{bmatrix} + \mathbf{E}^{\mathbf{T}} \lambda -$$

$$\mathbf{B}^T \begin{bmatrix} \mu_1 \\ \mu_2 \end{bmatrix} = \mathbf{0} \tag{4.106}$$

where

$$M_{11} = \left[m_1{}^L \frac{L_1{}^2}{4} + I_{1zz}\right] + m_3{}^L L_1{}^2 + m_3{}^L L_1 L_3 c\theta_3 + \left[m_3{}^L \frac{L_3{}^2}{4} + I_{3zz}\right] + m_5{}^L L_1{}^2 + m_5{}^L L_3{}^2 + [m_5{}^L g_5{}^2 + I_{5zz}] + 2m_5{}^L L_1 L_3 c\theta_3 + 2m_5{}^L L_1 g_5 c(\theta_3 + \theta_5 + \beta) + 2m_5{}^L L_3 g_5 c(\theta_5 + \beta) + \left[m_3{}^A L_1{}^2 + I^r{}_{3zz}\right] \quad (4.107)$$

$$M_{13} = \frac{1}{2} m_3{}^L L_1 L_3 c\theta_3 + \left[m_3{}^L \frac{L_3{}^2}{4} + I_{3zz}\right] + m_5{}^L L_3{}^2 + [m_5{}^L g_5{}^2 + I_{5zz}] + m_5{}^L L_1 L_3 c\theta_3 + m_5{}^L L_1 g_5 c(\theta_3 + \theta_5 + \beta) + 2m_5{}^L L_3 g_5 c(\theta_5 + \beta) \quad (4.108)$$

$$M_{15} = [m_5{}^L g_5{}^2 + I_{5zz}] + m_5{}^L L_1 g_5 c(\theta_3 + \theta_5 + \beta) + m_5{}^L L_3 g_5 c(\theta_5 + \beta) \quad (4.109)$$

$$M_{22} = \left[m_2{}^L \frac{L_2{}^2}{4} + I_{2zz}\right] + m_4{}^L L_2{}^2 + m_4{}^L L_2 L_4 c\theta_4 + \left[m_4{}^L \frac{L_4{}^2}{4} + I_{4zz}\right] \quad (4.110)$$

$$M_{24} = \frac{1}{2} m_4{}^L L_2 L_4 c\theta_4 + \left[m_4{}^L \frac{L_4{}^2}{4} + I_{4zz}\right] \quad (4.111)$$

$$M_{33} = \left[m_3{}^L \frac{L_3{}^2}{4} + I_{3zz}\right] + m_5{}^L L_3{}^2 + [m_5{}^L g_5{}^2 + I_{5zz}] + 2m_5{}^L L_3 g_5 c(\theta_5 + \beta) \quad (4.112)$$

$$M_{35} = [m_5{}^L g_5{}^2 + I_{5zz}] + m_5{}^L L_3 g_5 c(\theta_5 + \beta) \quad (4.113)$$

$$M_{44} = \left[m_4{}^L \frac{L_4{}^2}{4} + I_{4zz}\right] \quad (4.114)$$

$$M_{55} = [m_5{}^L g_5{}^2 + I_{5zz}] \quad (4.115)$$

$$Q_1 = {m_1}^L g\left(\frac{L_1}{2}c\theta_1\right) + {m_3}^L g\left(L_1 c\theta_1 + \frac{L_3}{2}c\theta_{13}\right) + {m_5}^L g[L_1 c\theta_1 + L_3 c\theta_{13} + g_5 c(\theta_{135} + \beta)] + {m_3}^A g L_1 c\theta_1 \quad (4.116)$$

$$Q_2 = {m_2}^L g\left(\frac{L_2}{2}c\theta_2\right) + {m_4}^L g\left(L_2 c\theta_2 + \frac{L_4}{2}c\theta_{24}\right) \quad (4.117)$$

$$Q_3 = \frac{1}{2}{\dot{\theta}_1}^2[{m_3}^L L_1 L_3 s\theta_3 + 2{m_5}^L L_1 L_3 s\theta_3 + 2{m_5}^L L_1 g_5 s(\theta_{35} + \beta)] + \dot{\theta}_1\dot{\theta}_3\left[\frac{1}{2}{m_3}^L L_1 L_3 s\theta_3 + {m_5}^L L_1 L_3 s\theta_3 + {m_5}^L L_1 g_5 s(\theta_{35} + \beta)\right] + \dot{\theta}_1\dot{\theta}_5[{m_5}^L L_1 g_5 s(\theta_{35} + \beta)] + {m_3}^L g\left(\frac{L_3}{2}c\theta_{13}\right) + {m_5}^L g[L_3 c\theta_{13} + g_5 c(\theta_{135} + \beta)] \quad (4.118)$$

$$Q_4 = \frac{1}{2}{\dot{\theta}_2}^2 {m_4}^L L_2 L_4 s\theta_4 + \dot{\theta}_2\dot{\theta}_4\frac{1}{2}{m_4}^L L_2 L_4 s\theta_4 + {m_2}^L g\left(\frac{L_2}{2}c\theta_2\right) + {m_4}^L g\left(L_2 c\theta_2 + \frac{L_4}{2}c\theta_{24}\right) \quad (4.119)$$

$$Q_5 = {\dot{\theta}_1}^2[{m_5}^L L_1 g_5 s(\theta_{35} + \beta) + {m_5}^L L_3 g_5 s(\theta_5 + \beta)] + {\dot{\theta}_3}^2 {m_5}^L L_3 g_5 s(\theta_5 + \beta) + \dot{\theta}_1\dot{\theta}_3\left[{m_5}^L L_1 g_5 s(\theta_{35} + \beta) + 2{m_5}^L L_3 g_5 s(\theta_5 + \beta)\right] + \dot{\theta}_1\dot{\theta}_5[{m_5}^L L_1 g_5 s(\theta_{35} + \beta) + {m_5}^L L_3 g_5 s(\theta_5 + \beta)] + \dot{\theta}_3\dot{\theta}_5 {m_5}^L L_3 g_5 s(\theta_5 + \beta) + {m_5}^L g[g_5 c(\theta_{135} + \beta)] \quad (4.120)$$

$$Da_1 = D_1\left(\dot{\theta}_1 - \dot{\phi}_1\right) \quad (4.121)$$

$$Da_2 = D_2\left(\dot{\theta}_2 - \dot{\phi}_2\right) \quad (4.122)$$

$$Da_3 = D_3\left(\dot{\theta}_3 - \dot{\phi}_3\right) \quad (4.123)$$

$$Da_4 = (D_4 + D_6)\dot{\theta}_4 - D_6\dot{\theta}_5 \quad (4.124)$$

$$Da_5 = -D_6\dot{\theta}_4 + (D_5 + D_6)\dot{\theta}_5 \tag{4.125}$$

$$St_1 = K_1(\theta_1 - \phi_1) \tag{4.126}$$

$$St_2 = K_2(\theta_2 - \phi_2) \tag{4.127}$$

$$St_3 = K_3(\theta_3 - \phi_3) \tag{4.128}$$

$$St_4 = 0 \tag{4.129}$$

$$St_5 = 0 \tag{4.130}$$

The system equations of motion corresponding to the second set of generalized coordinates can be written in matrix form as

$$\begin{bmatrix} I_{11} & 0 & 0 \\ 0 & I_{22} & 0 \\ 0 & 0 & I_{33} \end{bmatrix} \begin{bmatrix} \ddot{\phi}_1 \\ \ddot{\phi}_2 \\ \ddot{\phi}_3 \end{bmatrix} + \begin{bmatrix} D^r{}_1\dot{\phi}_1 \\ D^r{}_2\dot{\phi}_2 \\ D^r{}_3\dot{\phi}_3 \end{bmatrix} - \begin{bmatrix} D_1(\dot{\theta}_1 - \dot{\phi}_1) \\ D_2(\dot{\theta}_2 - \dot{\phi}_2) \\ D_3(\dot{\theta}_3 - \dot{\phi}_3) \end{bmatrix} - \begin{bmatrix} K_1(\theta_1 - \phi_1) \\ K_2(\theta_2 - \phi_2) \\ K_3(\theta_3 - \phi_3) \end{bmatrix} = \begin{bmatrix} T_1 \\ T_2 \\ T_3 \end{bmatrix} \tag{4.131}$$

where $\mathbf{D^r} = diag[D_i^r {r_i}^2]$ for $i = 1,2,3$.

It is required to write the equation of motion for the first set of generalized coordinates in terms of actuated variables as mentioned in Chapter III. Equations of motion can be written in two parts as shown below.

$$\mathbf{M^{aa}\ddot{q} + M^{au}\ddot{\theta}^u + Q^a + D^a(\dot{q} - \dot{\phi}) + K(q - \phi) - B^{a^T}\mu + E^{*^T}\lambda = 0} \tag{4.132}$$

where $\mathbf{D^a} = diag[D_i]$, $\mathbf{K} = diag[K_i]$ for $i = 1,2,3$

and

$$\mathbf{M^{aa}} = \begin{bmatrix} M_{11} & 0 & M_{13} \\ 0 & M_{22} & 0 \\ M_{31} & 0 & M_{33} \end{bmatrix} \tag{4.133}$$

$$\mathbf{M^{au}} = \begin{bmatrix} 0 & M_{15} \\ M_{24} & 0 \\ 0 & M_{35} \end{bmatrix} \tag{4.134}$$

$$\mathbf{Q^{aT}} = [Q_1 \quad Q_2 \quad Q_3] \tag{4.135}$$

$$\mathbf{M^{auT}\ddot{q} + M^{uu}\ddot{\theta}^u + Q^u + R\dot{\theta}^u - B^{uT}\mu = 0} \tag{4.136}$$

where

$$\mathbf{M^{uu}} = \begin{bmatrix} M_{44} & 0 \\ 0 & M_{55} \end{bmatrix} \tag{4.137}$$

$$\mathbf{Q^{uT}} = [Q_4 \quad Q_5] \tag{4.138}$$

$$\mathbf{R} = \begin{bmatrix} D_4 + D_6 & -D_6 \\ -D_6 & D_5 + D_6 \end{bmatrix} \tag{4.139}$$

Using Equations 2.58 and 2.59 for elimination of unactuated joint variables and solving Equation 4.136 for the Lagrange multipliers $\boldsymbol{\mu}$ and inserting into Equation 4.132 yields

$$\mathbf{M^*\ddot{q} + Q^* + D^a(\dot{q} - \dot{\phi}) + R^*\dot{q} + K(q - \phi) + E^{*T}\lambda = 0} \tag{4.140}$$

R* is derived similar to the derivation of **E*** and **P*** as explained in Chapter 3 and expressed as

$$\mathbf{R^* = R^a - R^u(B^u)^{-1}B^a} \tag{4.141}$$

4.2 Control Simulation and Results

The performance of the control law is checked by using MATLAB® software. All system constants and variables are defined and an *m-file* is written which performs the operations to calculate the control torques at each sampling time.

For the solution of Equations 3.40 and 3.41, functional iteration is used. Equations 3.40 and 3.41 are written as

$$\dot{\mathbf{q}}_{\mathbf{k+1}} = \begin{bmatrix} \mathbf{E}^* \frac{1}{h} + \dot{\mathbf{E}}^* \\ \mathbf{P}^* \frac{1}{h} + \dot{\mathbf{P}}^* \end{bmatrix}^{-1} \begin{bmatrix} \mathbf{E}^* \frac{1}{h} \dot{\mathbf{q}}_{\mathbf{k}} - \dot{\mathbf{G}} \\ \mathbf{P}^* \frac{1}{h} \dot{\mathbf{q}}_{\mathbf{k}} - \dot{\mathbf{H}} + \mathbf{z}_{\mathbf{k+1}} \end{bmatrix} \tag{4.142}$$

In the right hand side, initial value for $\dot{\mathbf{q}}_{\mathbf{k+1}}$ is $\dot{\mathbf{q}}_{\mathbf{k}}$ and Equation 4.142 is solved for new $\dot{\mathbf{q}}_{\mathbf{k+1}}$. Iteration continues until the norm of difference in $\dot{\mathbf{q}}_{\mathbf{k+1}}$ between successive iterations is less than ε. In the simulations, maximum 5 iterations were needed for $\varepsilon = 10^{-10}$.

After calculation of the control torques for each sampling time, the control torques are applied to the actual system which can be expressed as below.

$$\begin{bmatrix} \mathbf{M}^* & \mathbf{0} & \mathbf{E}^{*\mathbf{T}} \\ \mathbf{0} & \mathbf{I}^{\mathbf{r}} & \mathbf{I} \\ \mathbf{E}^* & \mathbf{0} & \mathbf{0} \end{bmatrix} \begin{bmatrix} \ddot{\mathbf{q}} \\ \ddot{\boldsymbol{\phi}} \\ \boldsymbol{\lambda} \end{bmatrix} = \begin{bmatrix} -\mathbf{Q}^* - \mathbf{D}(\dot{\mathbf{q}} - \dot{\boldsymbol{\phi}}) - \mathbf{K}(\mathbf{q} - \boldsymbol{\phi}) \\ \mathbf{T} - \mathbf{D}^{\mathbf{r}}\dot{\boldsymbol{\phi}} + \mathbf{D}(\dot{\mathbf{q}} - \dot{\boldsymbol{\phi}}) + \mathbf{K}(\mathbf{q} - \boldsymbol{\phi}) \\ -\dot{\mathbf{E}}^*\dot{\mathbf{q}} - \dot{\mathbf{G}} \end{bmatrix} \tag{4.143}$$

Joint and rotor accelerations are solved from Equation 4.14 and numerically integrated to obtain the measured joint and rotor positions and velocities. There is no need to measure the contact forces since it can be calculated as explained in previous sections.

Performance of the control law is checked for two groups of simulations. For each group, simulations including only the initial error, and simulations including both initial and modeling errors are performed. Modeling error is considered by setting the manipulator inertia and mass properties, the torsional spring constants and the damping constants 10% larger in the model.

The geometric data and the mass, inertial properties and gear ratios used in the simulations are shown in Table 4.1 and Table 4.2.

Table 4.1 The Geometric Data

Symbol	Value	Symbol	Value
L_1	1.0 m	d_0	1.8
L_2	1.0 m	g_5	0.75
L_3	1.0 m	d_5	0.80
L_4	1.0 m	α	20 deg
L_5	1.5 m	β	7 deg

Table 4.2 The Mass, Inertial Properties and Gear Ratios

Symbol	Value	Symbol	Value
m_1^L	10 kg	m_3^A	1.2 kg
m_2^L	10 kg	I^r_{1zz}	7.0e-05 kg.m^2
m_3^L	10 kg	I^r_{2zz}	8.0e-05 kg.m^2
m_4^L	10 kg	I^r_{3zz}	9.0e-05 kg.m^2
m_5^L	15 kg	r_1	100
m_1^A	1.2 kg	r_2	100
m_2^A	1.2 kg	r_3	100

Damping and spring constants are given in the table below.

Table 4.3 The Damping and Spring Constants

Symbol	**Value**	**Symbol**	**Value**
D_1	0.0355 N.m.s/rad	D^r_1	0.0003 N.m.s/rad
D_2	0.0379 N.m.s/rad	D^r_2	0.0003 N.m.s/rad
D_3	0.0402 N.m.s/rad	D^r_3	0.0003 N.m.s/rad
D_4	0.0200 N.m.s/rad	K_1	5000 N.m/rad
D_5	0.0200 N.m.s/rad	K_2	5000 N.m/rad
D_6	0.0200 N.m.s/rad	K_3	5000 N.m/rad

The system is initially at rest and the initial active joint positions are as follows.

$$\theta_{1_0} = 135° \tag{4.144}$$

$$\theta_{2_0} = 75° \tag{4.145}$$

$$\theta_{3_0} = -90° \tag{4.146}$$

This leads to the initial position of the end-effector as follows.

$$x_{1_0} = 0.6668 \text{ m} \tag{4.147}$$

$$x_{2_0} = 1.8563 \text{ m} \tag{4.148}$$

$$x_{3_0} = 0.2364 \text{ rad} = 13.55° \tag{4.149}$$

The desired motion and force trajectories are given below.

$$x_1^d = \begin{cases} 0.70 \text{ m} & 0 \le t < T_1 \\ 0.70 + \frac{0.5}{T}\left[t - T_1 - \frac{T}{2\pi} sin\frac{2\pi(t-T_1)}{T}\right] \text{ m} & T_1 \le t < T_1 + T \\ 1.20 \text{ m} & t \ge T_1 + T \end{cases} \tag{4.150}$$

$$x_3^d = \begin{cases} 15 \text{ deg} & 0 \le t < T_1 \\ 15 + \frac{15}{T}\left[t - T_1 - \frac{T}{2\pi} sin\frac{2\pi(t-T_1)}{T}\right] \text{ deg} & T_1 \le t < T_1 + T \\ 30 \text{ deg} & t \ge T_1 + T \end{cases} \tag{4.151}$$

$$\lambda^d = \begin{cases} 50\frac{t}{T_1} & 0 \le t < T_1 \\ 50 \text{ N} & T_1 \le t < T_1 + T \\ 50\left[1 - \frac{t-T_1-T}{T_2}\right] & T_1 + T \le t < T_1 + T + T_2 \\ 0 & t \ge T_1 + T + T_2 \end{cases} \tag{4.152}$$

where $T_1 = T_2 = 0.1$ s and $T = 0.5$ s.

It is assumed that the desired motion trajectory is out of singular positions.

The feedback gain diagonal matrices are chosen according to ITAE criteria and by using Table 3.1, $C_{1i} = 2.1\omega_i$, $C_{2i} = 3.4{\omega_i}^2$, $C_{3i} = 2.7{\omega_i}^3$, $C_{4i} = {\omega_i}^4$; $B_1 = 1.4\beta, B_2 = \beta^2$. ω_i and β are positive constants where i = 1,2. Sampling time interval is taken as h = 0.001.

First group of simulations are held with $\omega_i = 50$ rad/s and $\beta = 200$ rad/s. Second group of simulations are held with $\omega_i = 70$ rad/s and $\beta = 300$ rad/s.

Results are shown below.

First Group of Simulations

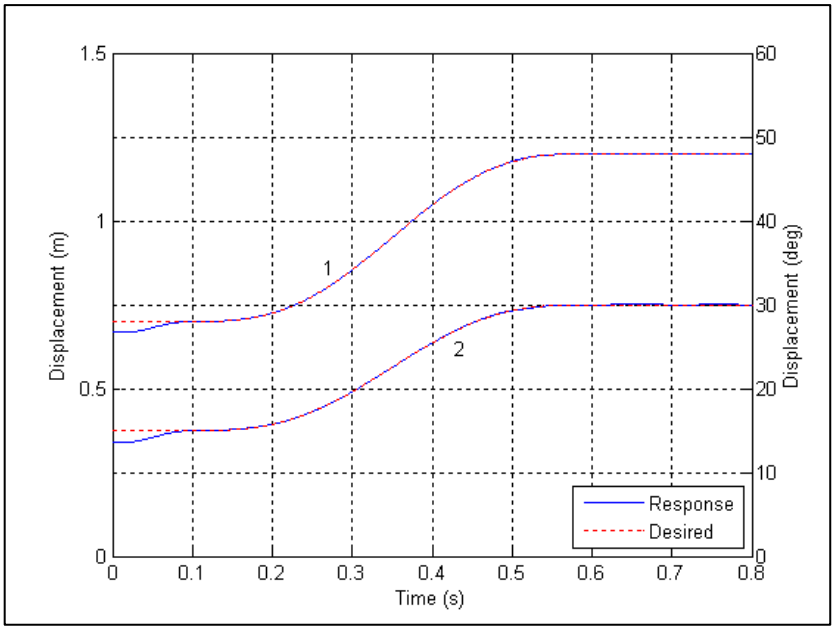

Figure 4.4 Position Response: 1. y_1, 2. y_3 ($\omega_i = 50$ rad/s, $\beta = 200$ rad/s)

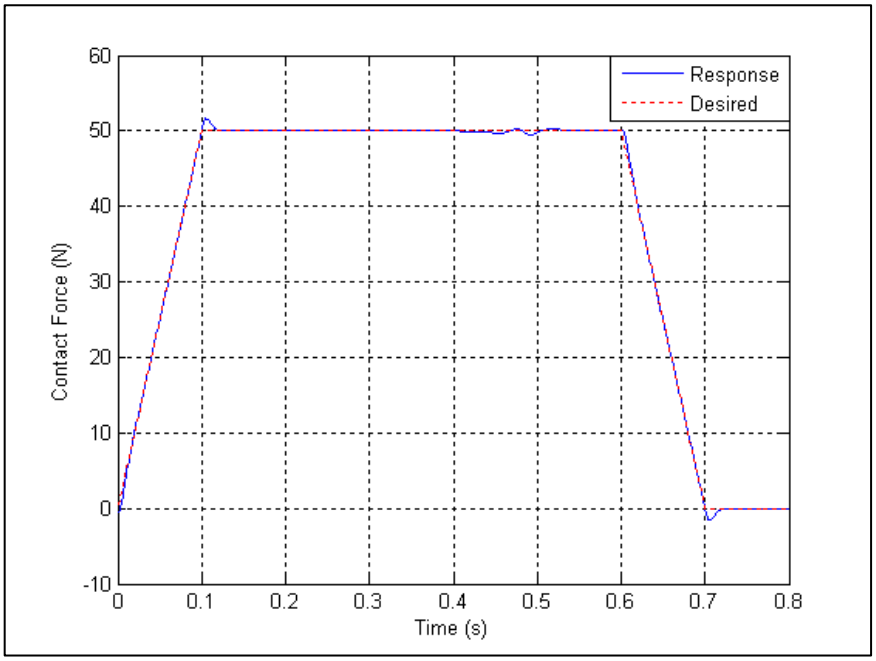

Figure 4.5 Contact Force Response ($\omega_i = 50$ rad/s, $\beta = 200$ rad/s)

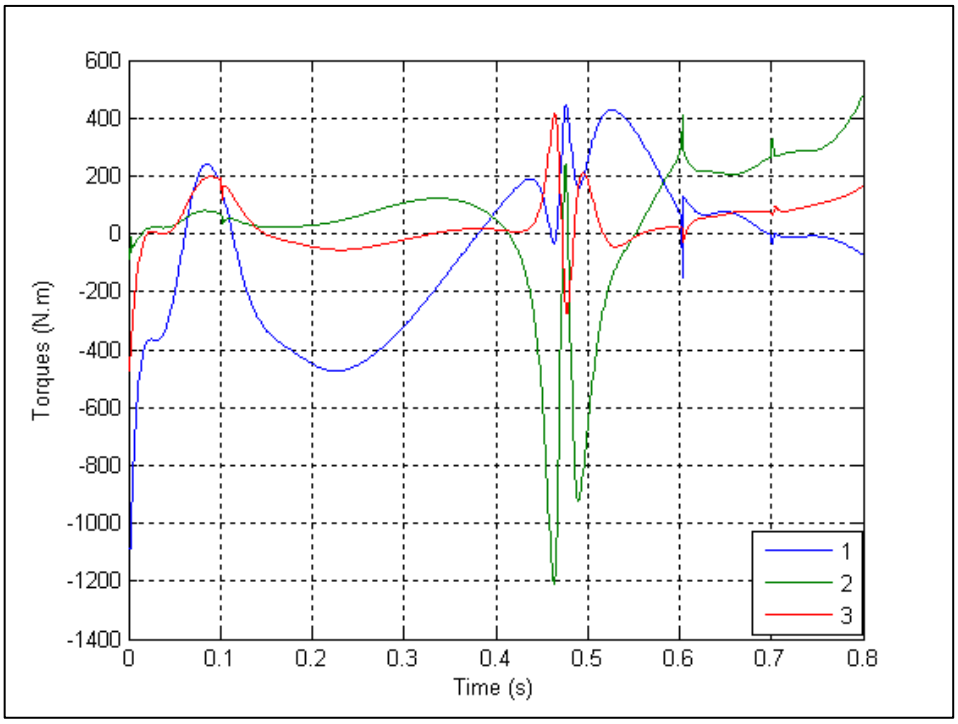

Figure 4.6 Control Torques: 1. T_1^a, 2. T_2^a, 3. T_3^a ($\omega_i = 50$ rad/s, $\beta = 200$ rad/s)

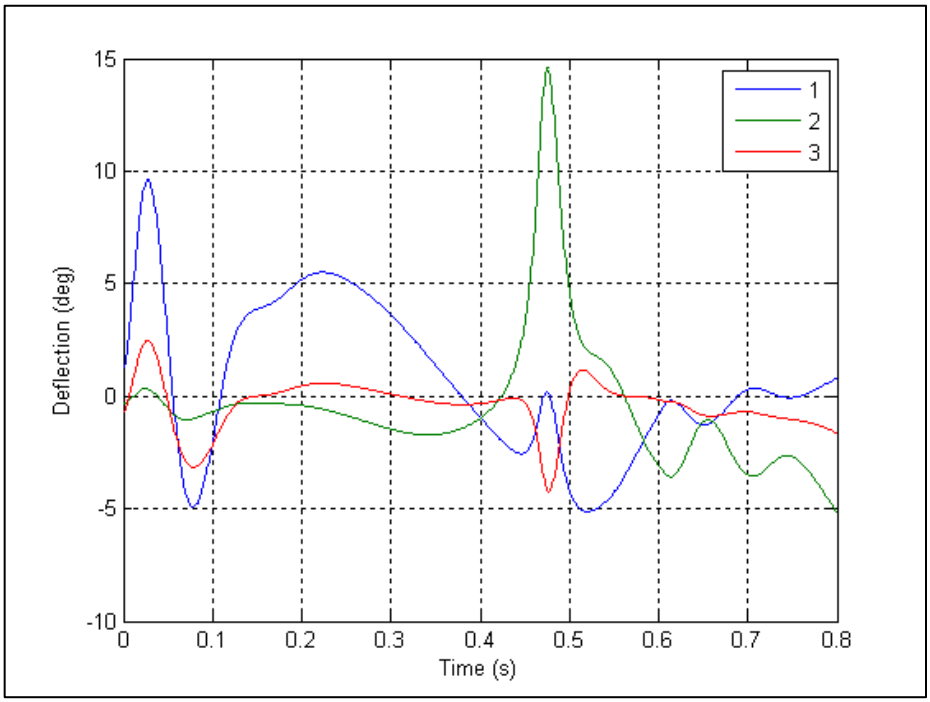

Figure 4.7 Elastic Deflections: 1. $\theta_1 - \Phi_1$, 2. $\theta_2 - \Phi_2$, 3. $\theta_3 - \Phi_3$ ($\omega_i = 50$ rad/s, $\beta = 200$ rad/s)

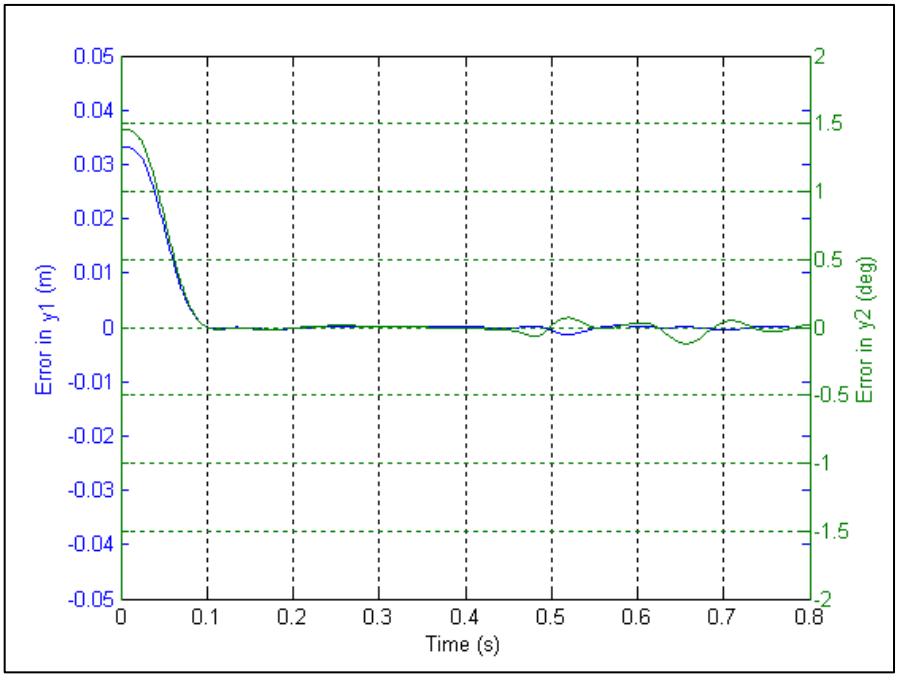

Figure 4.8 Position Errors (ω_i = 50 rad/s, β = 200 rad/s)

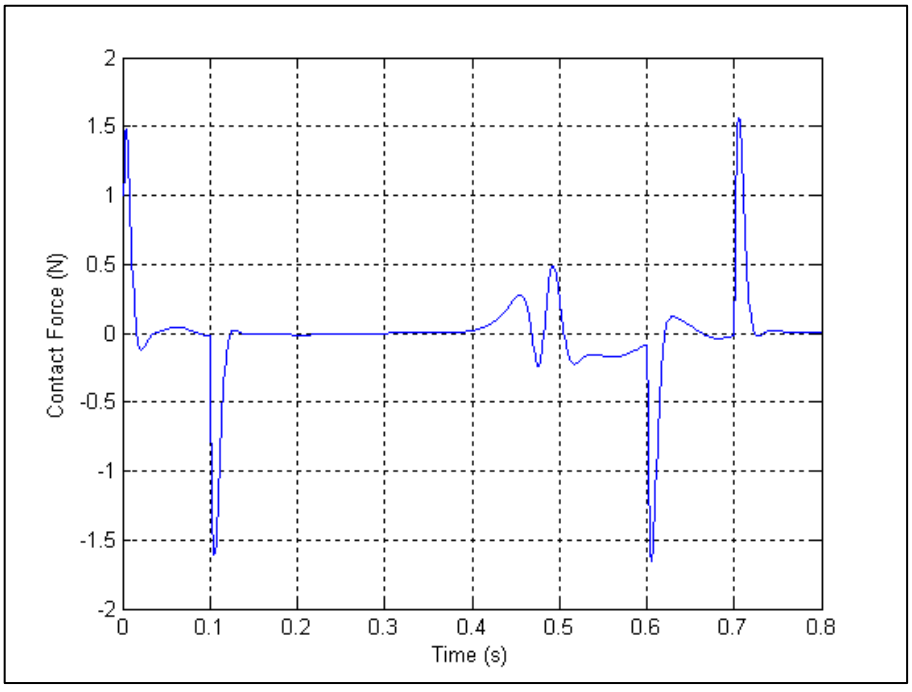

Figure 4.9 Contact Force Errors (ω_i = 50 rad/s, β = 200 rad/s)

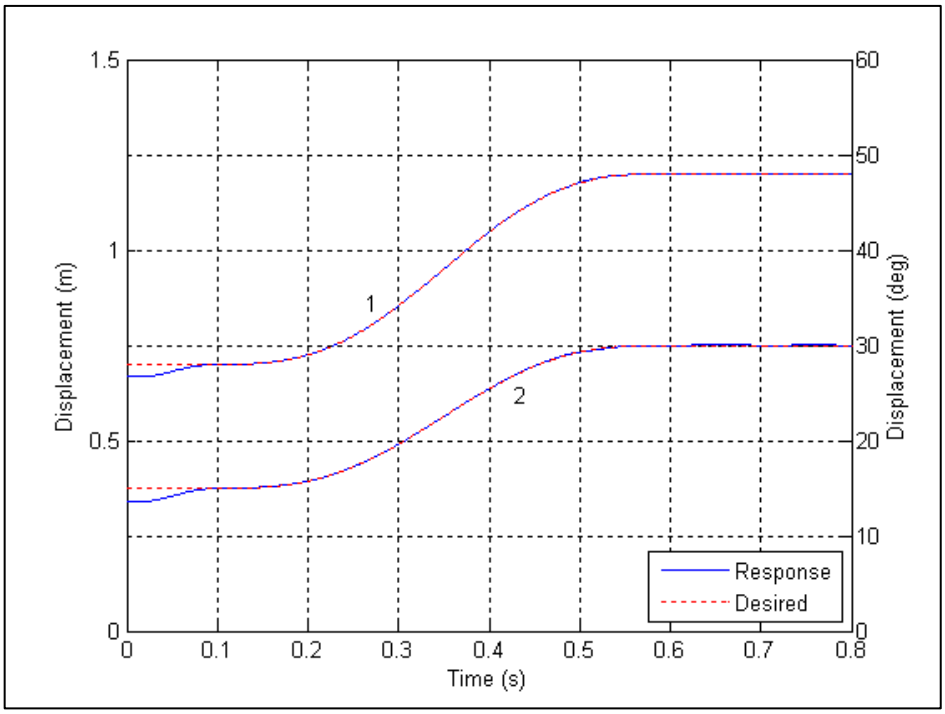

Figure 4.10 Position Response: 1. y_1, 2. y_2 (ω_i = 50 rad/s, β = 200 rad/s, Including Modeling Error)

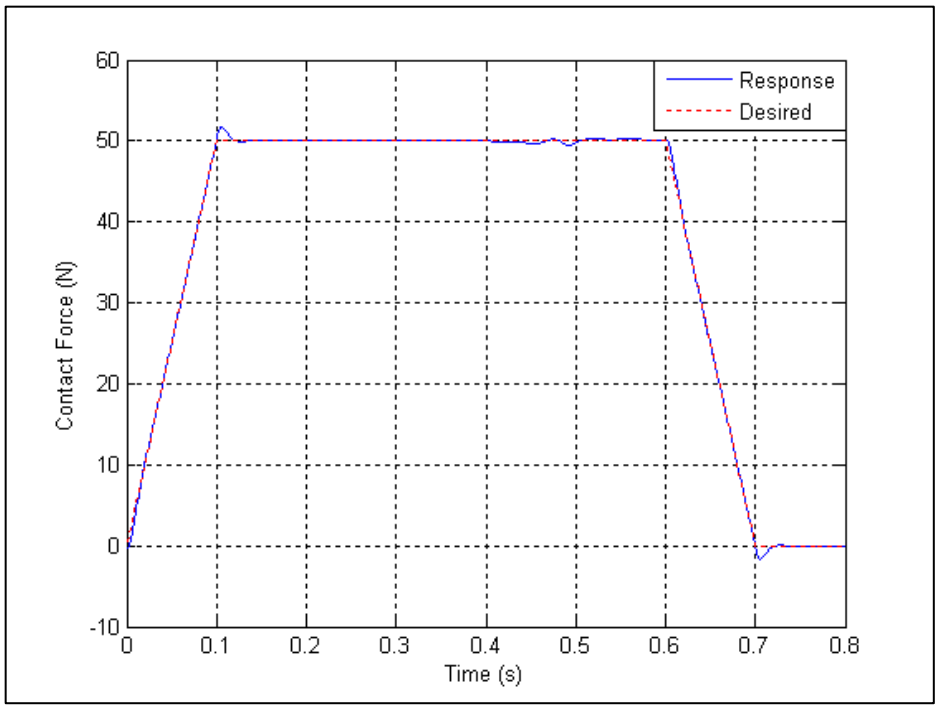

Figure 4.11 Contact Force Response (ω_i = 50 rad/s, β = 200 rad/s, Including Modeling Error)

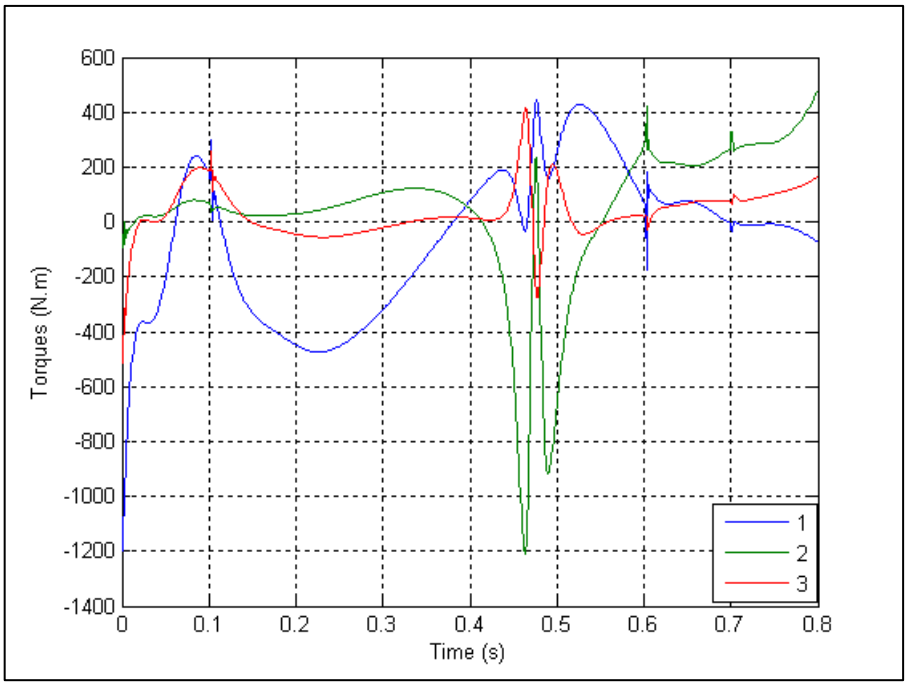

Figure 4.12 Control Torques: 1. T_1^a, 2. T_2^a, 3. T_3^a (ω_i = 50 rad/s, β = 200 rad/s, Including Modeling Error)

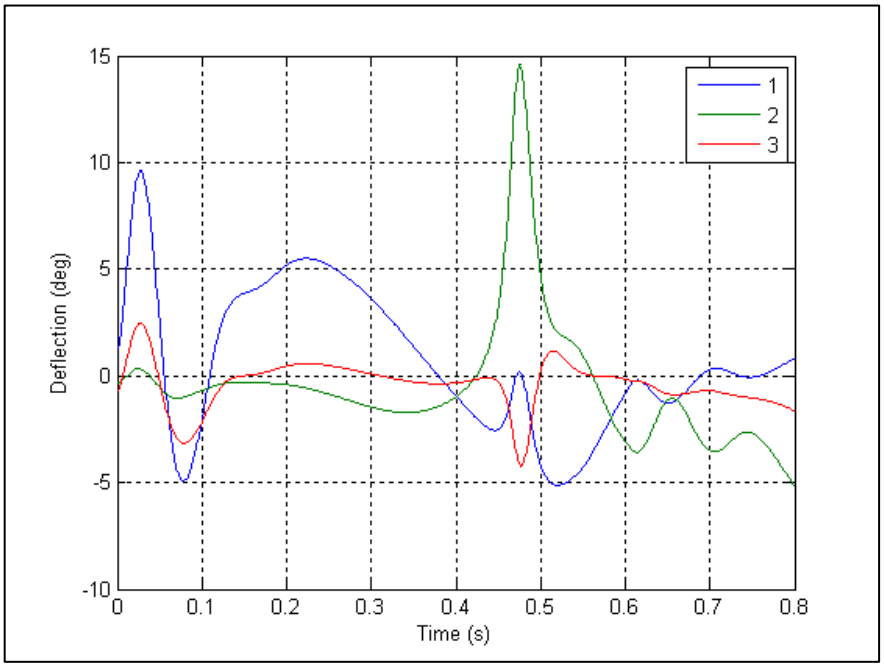

Figure 4.13 Elastic Deflections: 1. θ_1 - Φ_1, 2. $\theta_2 - \Phi_2$, 3. $\theta_3 - \Phi_3$ (ω_i = 50 rad/s, β = 200 rad/s, Including Modeling Error)

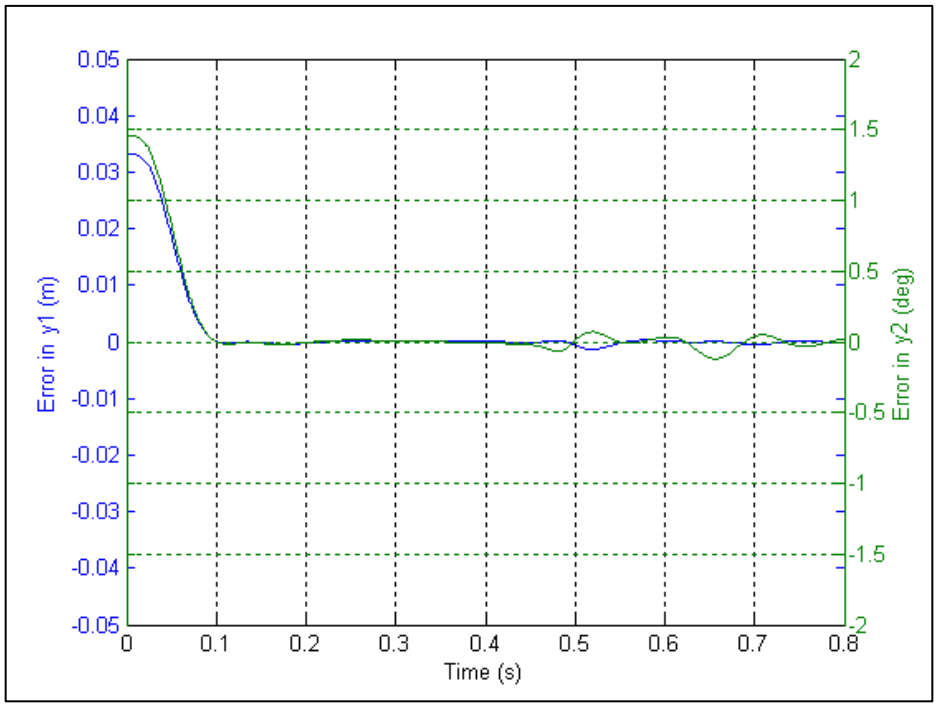

Figure 4.14 Position Errors (ω_i = 50 rad/s, β = 200 rad/s, Including Modeling Error)

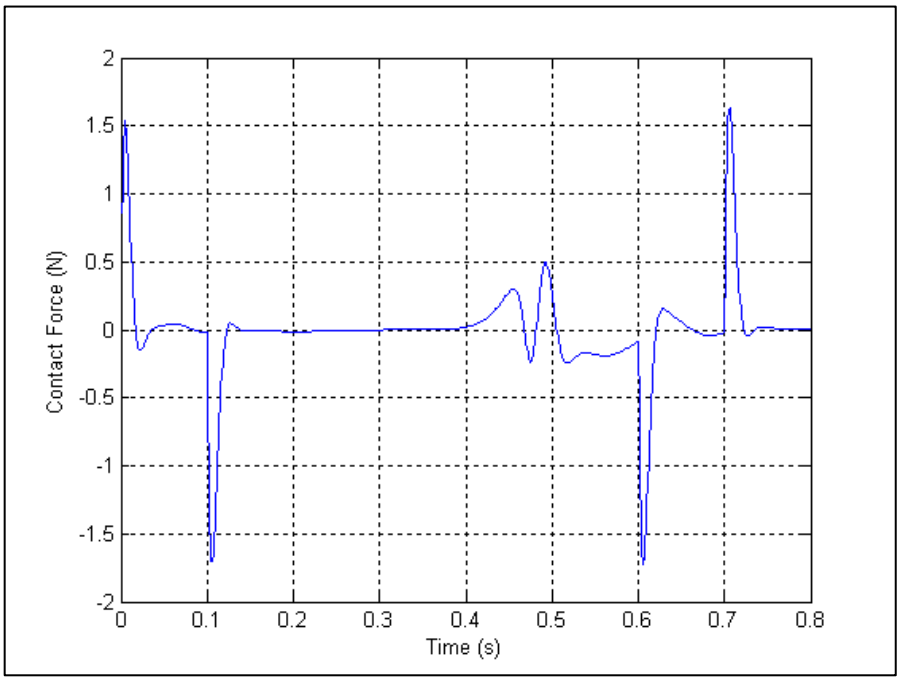

Figure 4.15 Contact Force Errors (ω_i = 50 rad/s, β = 200 rad/s, Including Modeling Error)

Second Group of Simulations

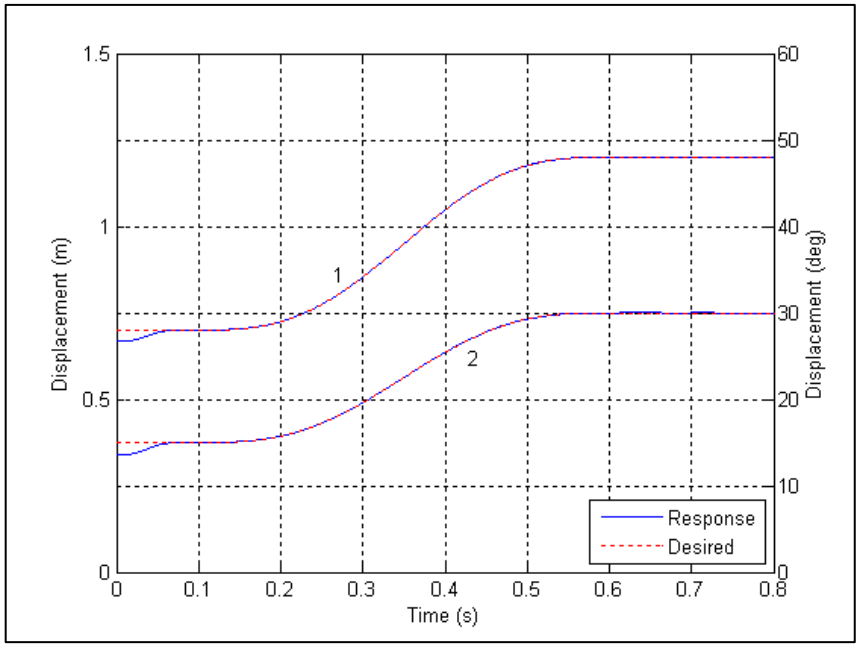

Figure 4.16 Position Response: 1. y_1, 2. y_2 (ω_i = 70 rad/s, β = 300 rad/s)

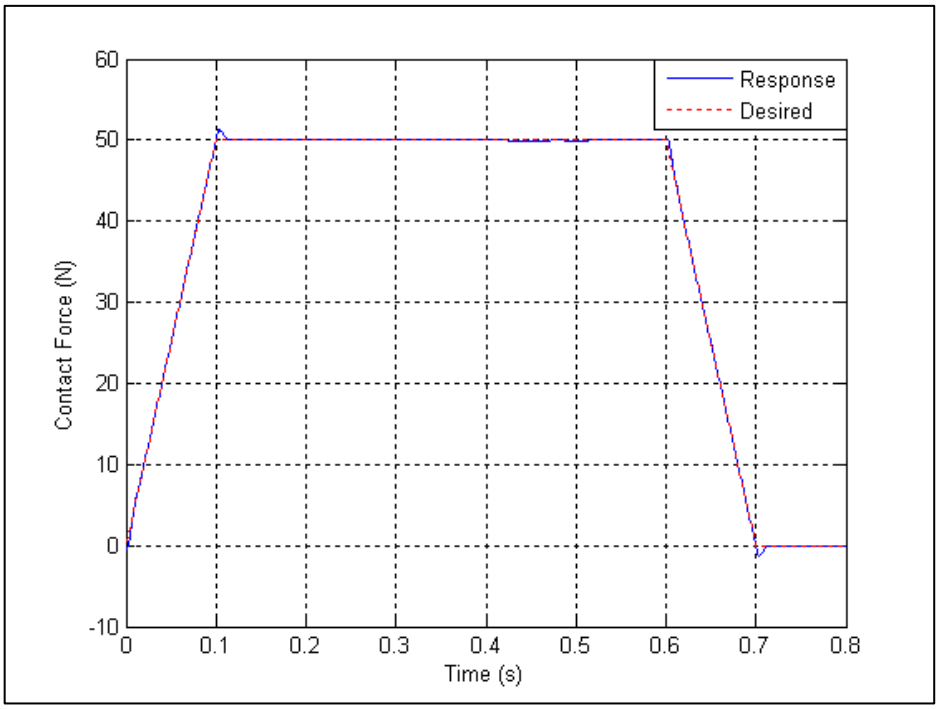

Figure 4.17 Contact Force Response (ω_i = 70 rad/s, β = 300 rad/s)

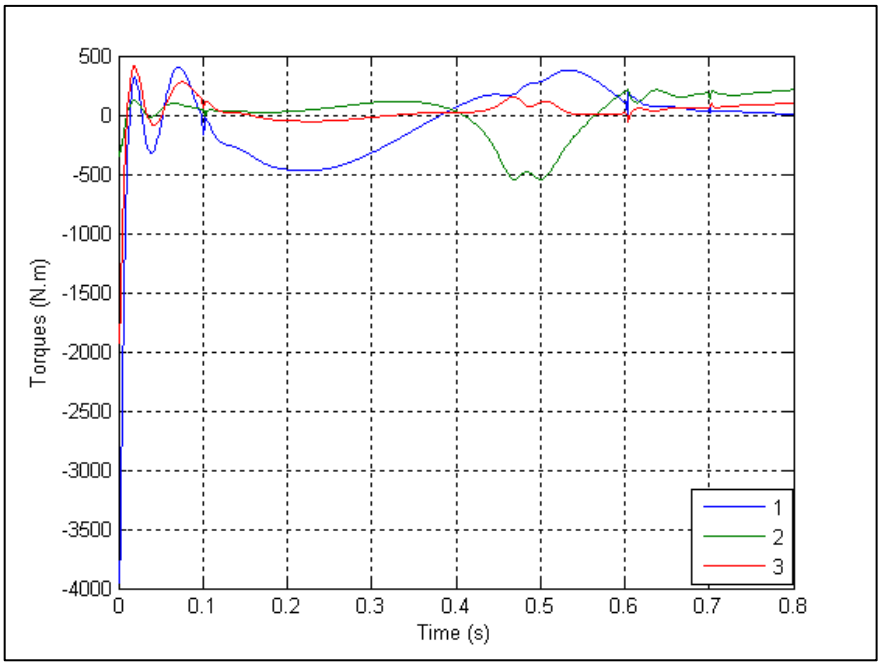

Figure 4.18 Control Torques: 1. T_1^a, 2. T_2^a, 3. T_3^a (ω_i = 70 rad/s, β = 300 rad/s)

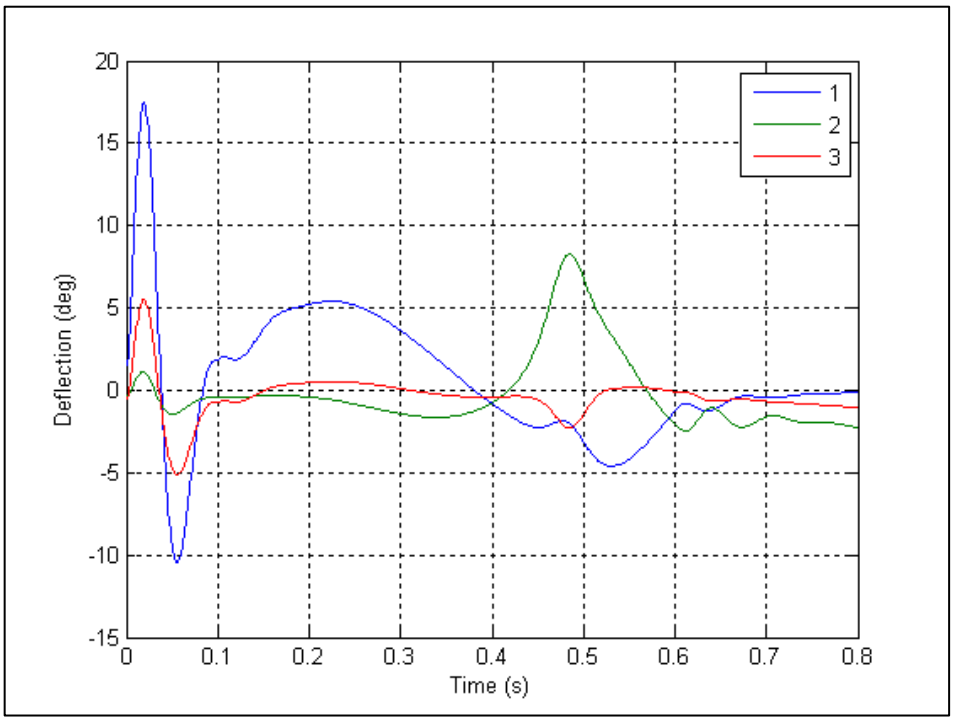

Figure 4.19 Elastic Deflections: 1. θ_1 - Φ_1, 2. $\theta_2 - \Phi_2$, 3. $\theta_3 - \Phi_3$ (ω_i = 70 rad/s, β = 300 rad/s)

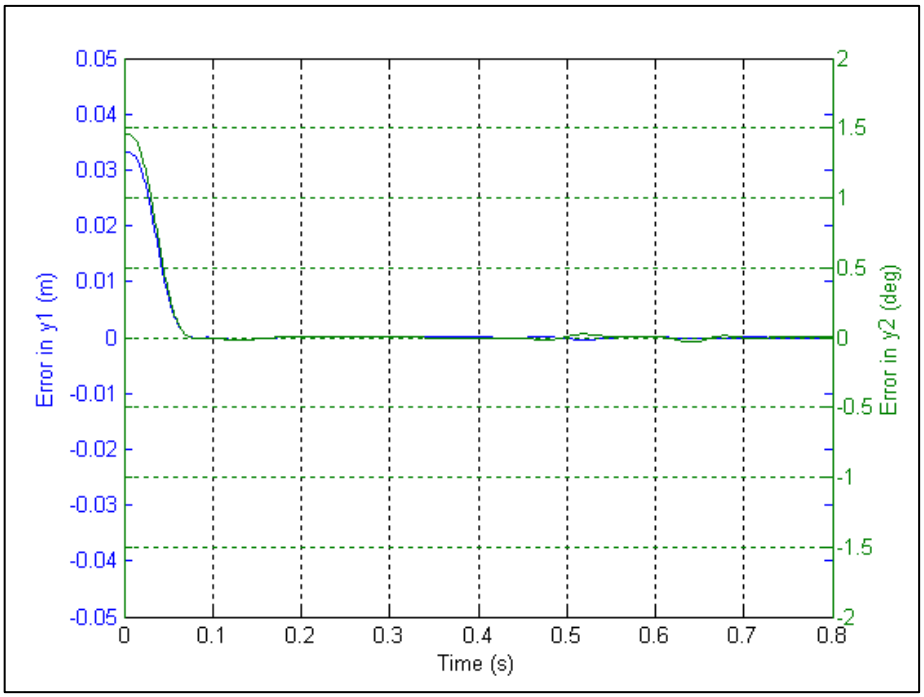

Figure 4.20 Position Errors (ω_i = 70 rad/s, β = 300 rad/s)

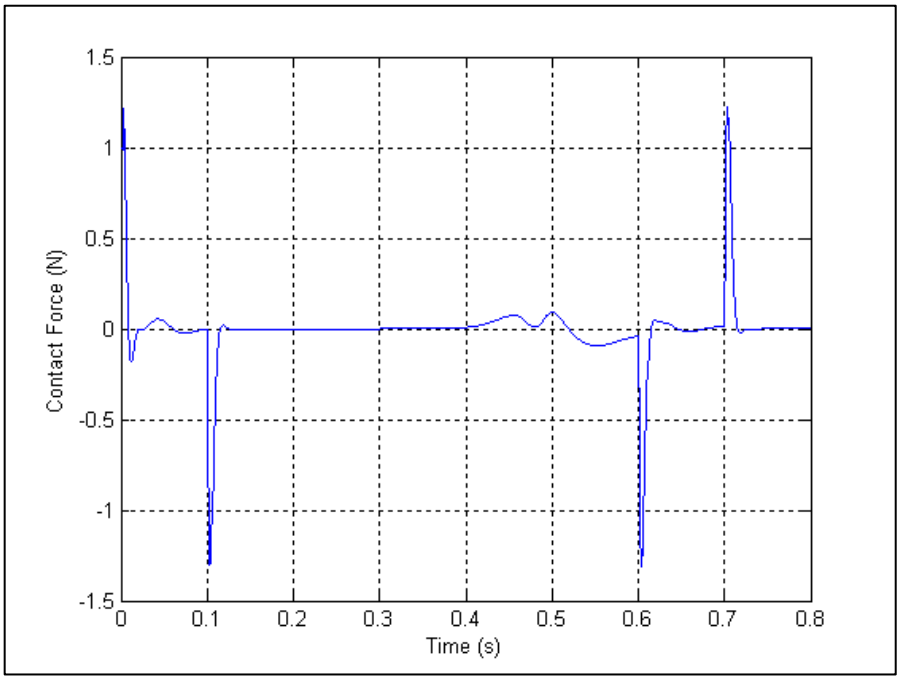

Figure 4.21 Contact Force Errors (ω_i = 70 rad/s, β = 300 rad/s)

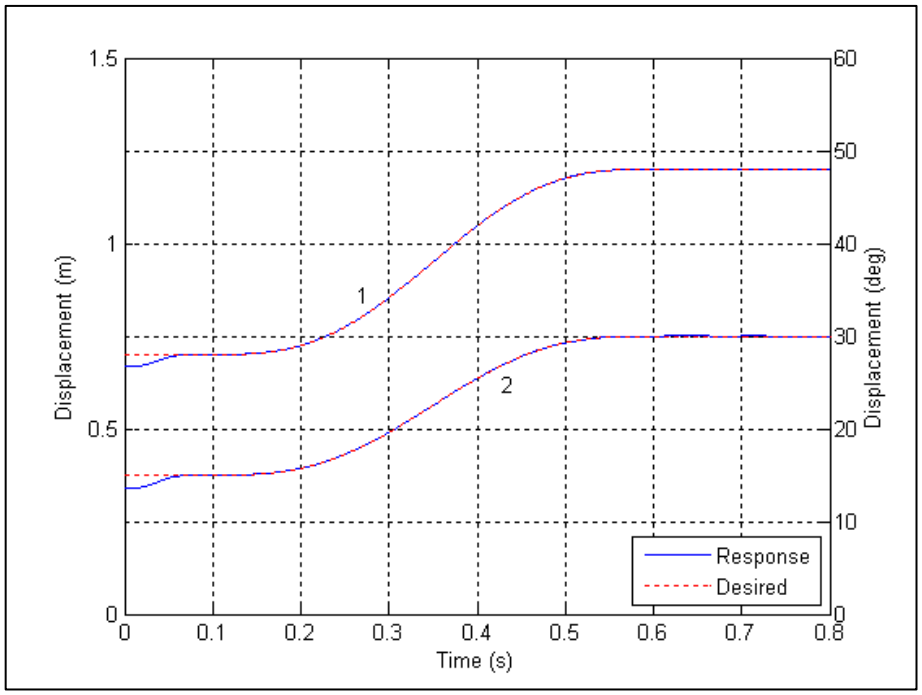

Figure 4.22 Position Response: 1. y_1, 2. y_2 , (ω_i = 70 rad/s, β = 300 rad/s, Including Modeling Error)

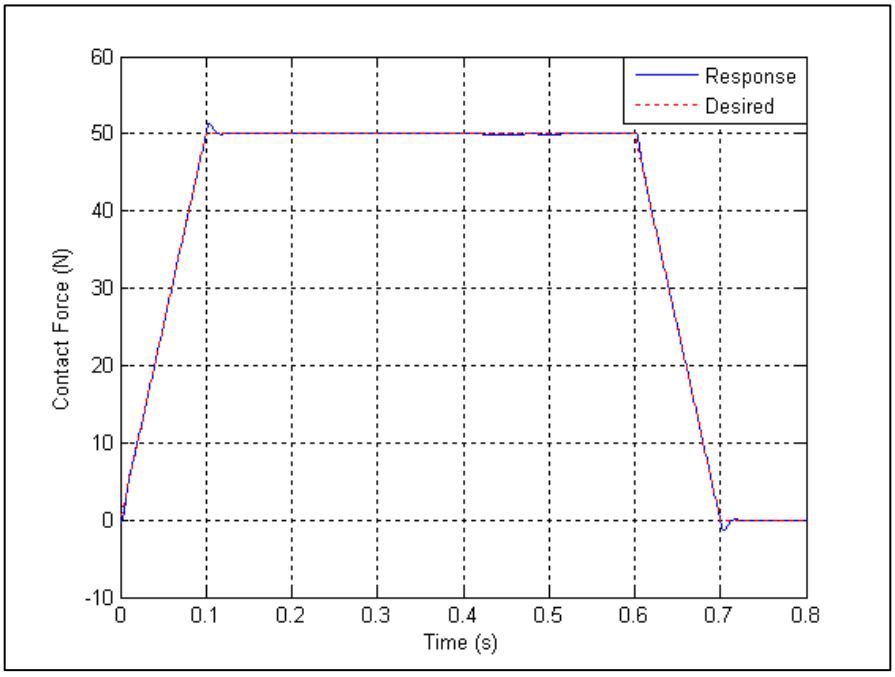

Figure 4.23 Contact Force Response (ω_i = 70 rad/s, β = 300 rad/s, Including Modeling Error)

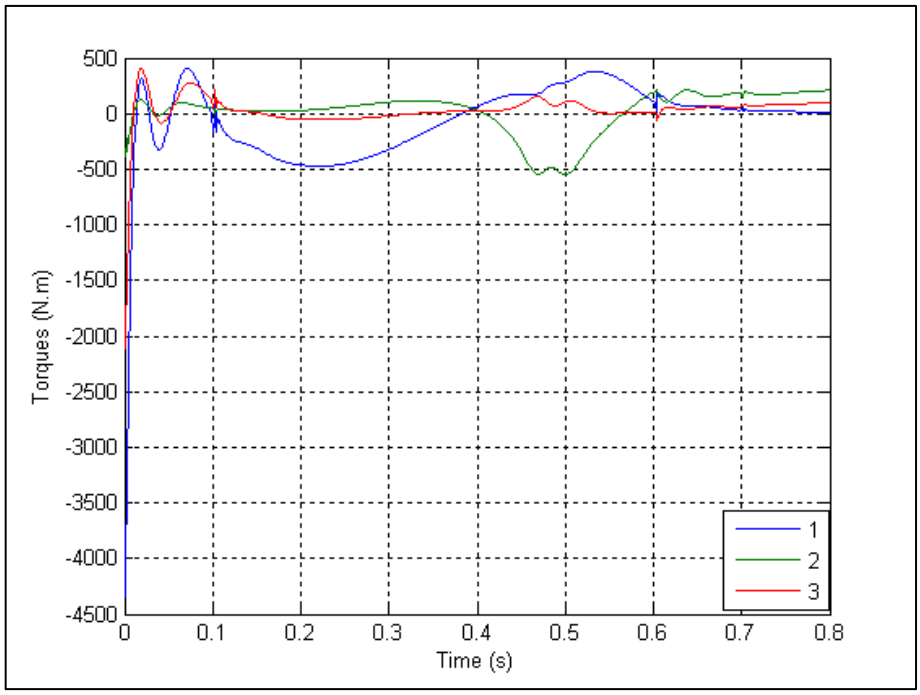

Figure 4.24 Control Torques: 1. T_1^a, 2. T_2^a, 3. T_3^a, (ω_i = 70 rad/s, β = 300 rad/s, Including Modeling Error)

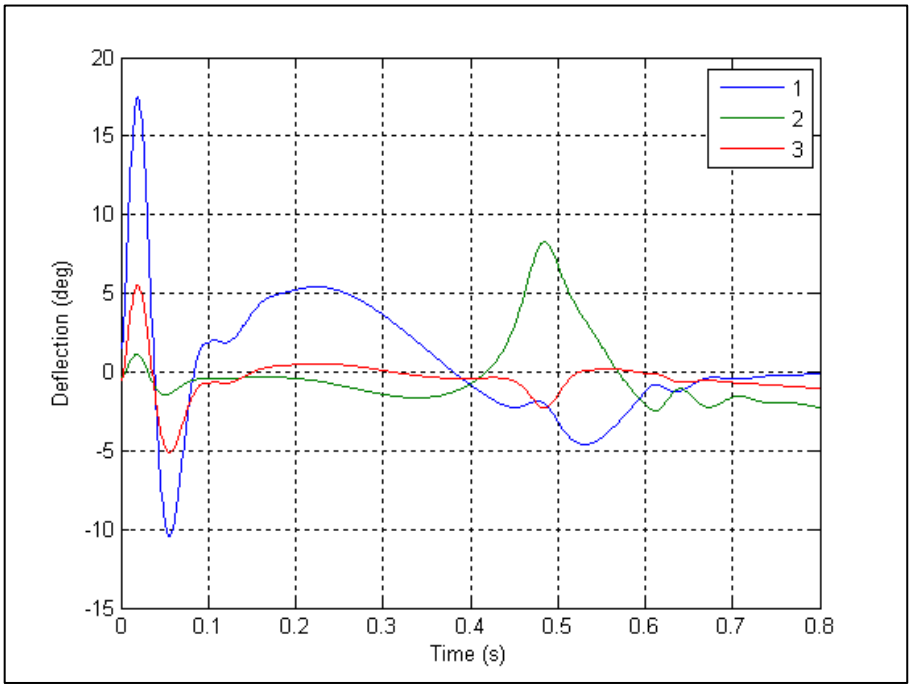

Figure 4.25 Elastic Deflections: 1. θ_1 - Φ_1, 2. $\theta_2 - \Phi_2$, 3. $\theta_3 - \Phi_3$, (ω_i = 70 rad/s, β = 300 rad/s, Including Modeling Error)

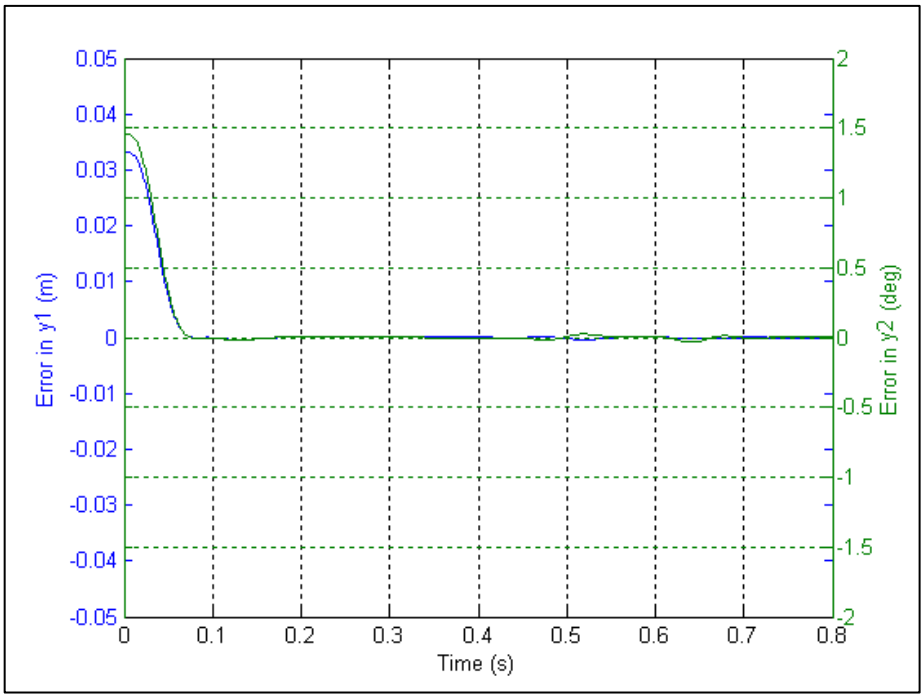

Figure 4.26 Position Errors, (ω_i = 70 rad/s, β = 300 rad/s, Including Modeling Error)

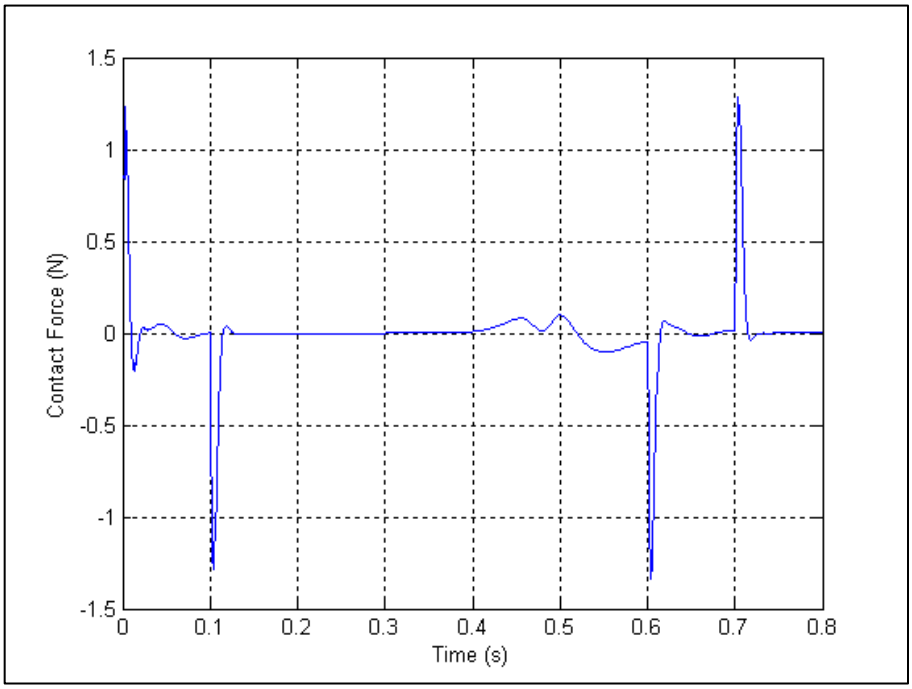

Figure 4.27 Contact Force Errors, (ω_i = 70 rad/s, β = 300 rad/s, Including Modeling Error)

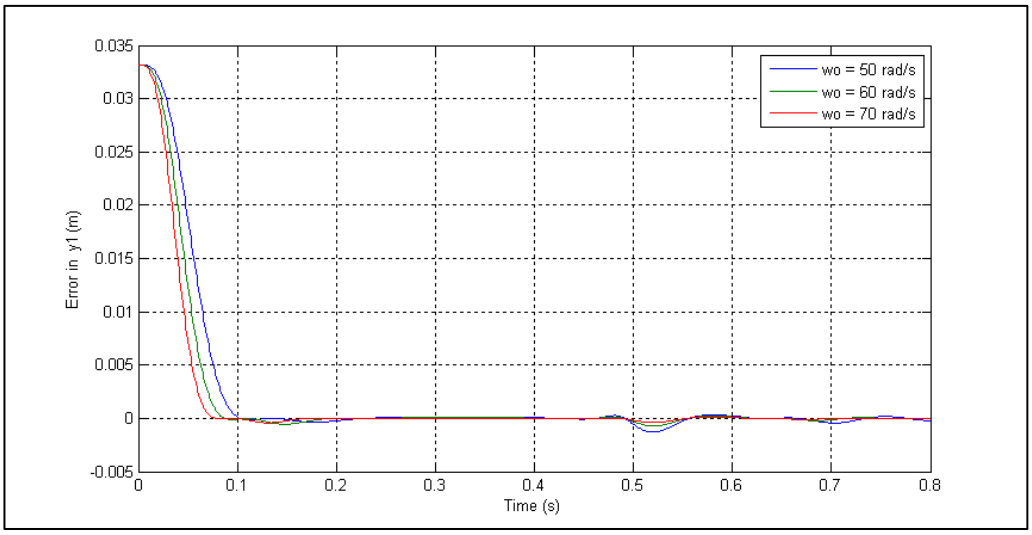

Figure 4.28 Effect of Feedback Gains on y_1

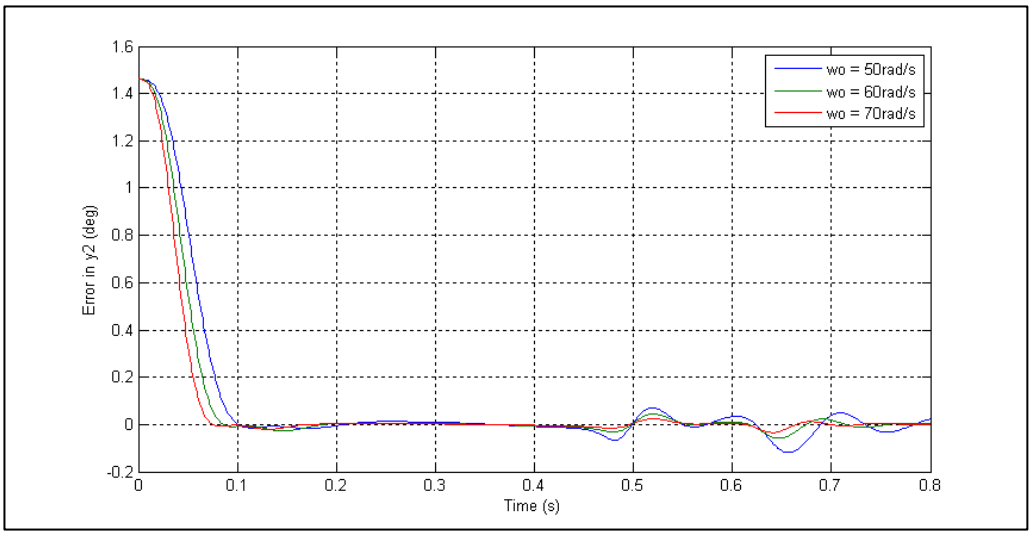

Figure 4.29 Effect of Feedback Gains on y_2

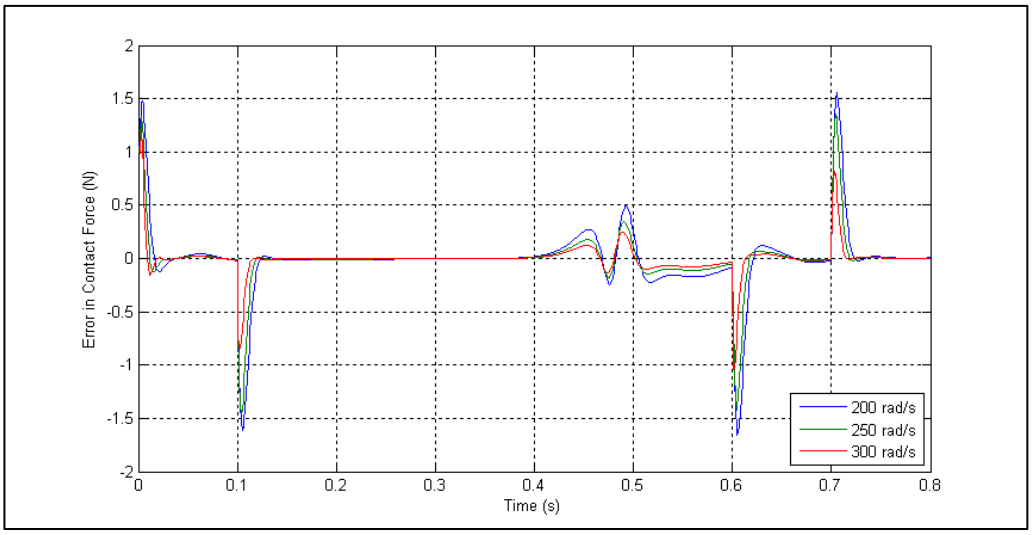

Figure 4.30 Effect of Feedback Gains on contact Forces

CHAPTER 5

DISCUSSIONS AND CONCLUSION

5.1 Discussions

The simulations are performed for two different simulation groups with different feedback gain constants. In the simulations where the modeling error is not considered while initial position error is taken into account, it is observed that good tracking performances are achieved for motion and the contact force. On the other hand, it is seen that initial position errors cause large initial control torques. As seen in Figures 4.28, 4.29 and 4.30, tracking errors are reduced by increasing ω_0 and β with the expense of larger control torques and larger elastic deflections. The initial and final elastic deflections are nonzero due to the gravitational forces.

For each group, the simulations are performed with considering both the initial and modeling errors as well. For this purpose, mass/inertia parameters, spring and damping constants are assumed to be 10 % larger in the model. No significant change is observed in tracking errors, control torques and elastic deflections. Control torques are increased at the discontinuities of the reference motion and force trajectories.

Steady state errors are obtained as $y_1 = -2.5 \times 10^{-4}$ m, $y_2 = 0.023$ *deg* and $\lambda = 0.0077$ N and $y_1 = -1.099 \times 10^{-5}$ m, $y_2 = 7.6 \times 10^{-4}$ *deg* and $\lambda = 9.2 \times 10^{-4}$ N for the first and second simulation groups simultaneously.

5.2 Conclusion

This thesis presented the hybrid force and motion trajectory tracking control law for flexible joint parallel manipulators based on solving the acceleration level inverse dynamic equations which are singular.

Further differentiations of equations of motion, constraint equations and task equations are avoided by the proposed method. This simplifies the calculations and reduces the complexity in equations. The only feedback variables are joint and actuator rotor positions and velocities. Since the constraint equation is defined, there is no need to measure the contact forces. Contact forces are found by appropriate calculations. However it must be noted that since the contact force is not measured, in practical applications, any unexpected change in the contact surface profile may result with inaccurate contact force feedback information.

The important point about the algorithm is that since control torques cannot make an instantaneous effect on the end-effector accelerations, end-effector jerks, end-effector contact forces and contact force rates, any jump in Γ, $\dot{\Gamma}$, $\mathbf{z}$, and $\dot{\mathbf{z}}$ require infinitely large control torques. To avoid this,Γ, $\dot{\Gamma}$, $\mathbf{z}$, and $\dot{\mathbf{z}}$ are matched at the discontinuities of the reference force and motion trajectories by freely selecting the integration constants.

Simulations are carried out for two simulation groups with different feedback gain constants. As a result, it is shown that good tracking properties are obtained for the desired force and motion trajectories by using the proposed control algorithm.

REFERENCES

[1] **Rivin E. I., (1984),** "Compliance Breakdown for Robot Structures", Proceedings of the Symposium Engineering Applied Mechanics, Toronto.

[2] **Good M.C, Sweet L.M., Strobel K.L (1985),** "Dynamic Models for Control System Design of Integrated Robot and Drive Systems", Journal of Dynamic Systems, Measurement and Control 107 pp. 53-59.

[3] **Spong M. W., (1987),** "Modeling and Control of Elastic Joint Robots", Journal of Dynamic Systems, Measurement and Control, Vol. 109, pp. 310-319.

[4] **Forrest-Barlach M. G., Babcock S. M., (1987),** "Inverse Dynamics Position Control of a Compliant Manipulator", IEEE Journal of Robotics and Automation, No.1, Vol. Ra-3, pp. 75-83.

[5] **Jankowski K. P., Van Brussel H., (1992),** "An Approach to Discrete Inverse Dynamics Control of Flexible Joint Robots", IEEE Transactions on Robotics and Automation, No.5, Vol. 8, pp. 651-658.

[6] **İder K. and Özgören K., (2000),** "Trajectory Tracking Control of Flexible Joint Robots", Computers and Structures, Vol. 76, pp. 757-763.

[7] **Hu Y.R., Vukovich G.,** "Position and force control of flexible joint robots during constrained motion tasks", Mechanism and Machine Theory 36 (2001) pp. 853-871

[8] **Jankowski K.P., H.A. Elmaraghy H.A.,** "Inverse Dynamics and feedforward controllers for high presicion position/force tracking of flexible joint robots" Robotica 12 (1994) pp. 227-241

[9] **İder K., (2000),** "Force and Motion trajectory Tracking control of Flexible Joint Robots", Mechanism and Machine Theory Vol 35, pp.363-378.

[10] **Korkmaz, O., (2006),** "Inverse Dynamics Control of Flexible Joint Parallel Manipulators", M.S. Thesis, Mechanical Engineering Department, Middle East Technical University, Ankara, Turkey

[11] **Ozgoli S., Taghirad H.D.**, "A survey on the control of flexible joint robots", Asian Journal of Control 8 (2006) 1-15

[12] **Dwivedya S.K., Eberhard P.,** Dynamic analysis of flexible manipulators, a literature review, Mechanism and Machine Theory Volume 41, Issue 7, July 2006, pp. 749-777

[13] **Ider K., Korkmaz O.,** "Trajectory tracking control of parallel robots in the presence of joint drive flexibility", Journal of Sound and Vibration 319 (2009) pp. 77-90

[14] **İyigün, H. H., (2001)**, "Inverse Dynamics Control of Constrained Flexible Joint Robots", M.S. Thesis, Mechanical Engineering Department, Middle East Technical University, Ankara, Turkey

[15] **Nagarth I.J, Gopal M. (2006),** "Control Systems Engineering", New Age International Publishers, pp. 223-237

[16] **Özgören K., (2005),** "ME522 Principles of Robotics Lecture Notes", Mechanical Engineering Department, Middle East Technical University, Ankara, Turkey.

[17] **İder K., (2007),** "ME 528 Flexible Multibody Dynamics Lecture Notes", Mechanical Engineering Department, Middle East Technical University, Ankara, Turkey.

[18] **The Mathworks Inc., (2007),** "Matlab User's Guide".